

**Forschungszentrum Karlsruhe**  
**in der Helmholtz-Gemeinschaft**

Wissenschaftliche Berichte  
FZKA 6761

*Kinetics of Water-Gas-Shift-Reaction  
using **MoS<sub>2</sub>** catalyst dotted with **Co***

H.J. Ederer, T. Fritsch, E. Henrich, C.E. Mas

Institut für Technische Chemie

Forschungszentrum Karlsruhe GmbH, Karlsruhe  
2002

**Impressum der Print-Ausgabe:**

**Als Manuskript gedruckt  
Für diesen Bericht behalten wir uns alle Rechte vor**

**Forschungszentrum Karlsruhe GmbH  
Postfach 3640, 76021 Karlsruhe**

**Mitglied der Hermann von Helmholtz-Gemeinschaft  
Deutscher Forschungszentren (HGF)**

**ISSN 0947-8620**

## Abstract

The kinetics of the water gas shift reaction and the inverse water gas shift reaction with Co dotted  $\text{MoS}_2$  catalyst has been investigated in a laboratory fixed bed apparatus. 266 experiments were performed with different temperatures, different pressures, different flow rates and different compositions. All the experiments can be described excellently with three different models and of course three different sets of parameters:

1. a global kinetics with fractional exponents
2. a standard Hinshelwood kinetics with adsorption-desorption equilibrium constants for all gases
3. a kinetics formulated as elementary reactions for the surface reaction, the adsorption and the desorption. The most simple Hinshelwood mechanism was the basis for our set of elementary reactions.

## Kinetik der Wassergas-Shift-Reaktion an einem $\text{MoS}_2$ Katalysator:

### Zusammenfassung

Die Kinetik der Wassergas Shift-Reaktion und der inversen Wassergas Shift-Reaktion mit einem Co dotierten  $\text{MoS}_2$  Katalysator wurde in einer Laborfestbettapparatur untersucht. Insgesamt 266 Experimente wurden durchgeführt. Dabei wurden verschiedene Temperaturen, verschiedene Flußgeschwindigkeiten, verschiedene Drucke und verschiedene Anfangszusammensetzungen als äußere Parameter gewählt. Alle Experimente können sehr gut mit drei verschiedenen Modellen beschrieben werden. Für jedes Modell wurde ein optimaler Parametersatz ermittelt, der alle Experimente gemeinsam beschreibt. Die drei verschiedenen Modelle sind:

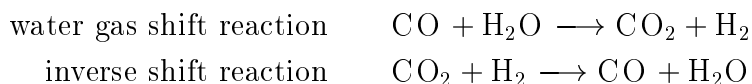
1. eine globale Kinetik mit gebrochenen Exponenten
2. eine übliche Hinshelwood Kinetik mit Adsorption-Desorptions Gleichgewichtskonstanten für alle Gase
3. eine mit Elementarreaktionen formulierte Kinetik. Diese Kinetik berücksichtigt alle Oberflächenreaktionen, alle Adsorptionsreaktionen und alle Desorptionsreaktionen, wie sie im einfachsten Hinshelwood Mechanismusansatz beschrieben werden.

# Contents

<b>1</b>	<b>Introduction</b>	<b>3</b>
<b>2</b>	<b>Experimental Design</b>	<b>3</b>
2.1	The catalyst . . . . .	3
2.2	The experimental fixed bed reactor . . . . .	5
2.3	Carrying out of the kinetic experiments . . . . .	7
<b>3</b>	<b>Results and Discussions</b>	<b>11</b>
3.1	Experimental results . . . . .	11
3.2	Experimental results with equimolar feed concentrations . . . . .	17
3.3	Global modelling with all experimental results . . . . .	20
3.4	Modelling with a catalytic standard model using all experimental results . . . . .	25
3.5	Modelling the Hinshelwood kinetics in the form of elementary reactions . . . . .	31
3.6	Catalyst poisoning . . . . .	37
<b>4</b>	<b>Appendices</b>	<b>37</b>
4.1	Catalyst activation and resulfidation . . . . .	37
4.2	Computer programs . . . . .	39
4.2.1	mechdiff.m . . . . .	39
4.2.2	shift02.txt . . . . .	42
4.2.3	dgl.m . . . . .	42
4.2.4	hauptprogramm.m . . . . .	44
4.2.5	zielfunktion.m . . . . .	45
4.2.6	caus.m . . . . .	46
	<b>References</b>	<b>47</b>

# 1 Introduction

The different gasification methods of biomass lead to a gas composition which has to be changed to be usable for the different applications like methanol synthesis or Fischer-Tropsch synthesis et cetera. The CO/H<sub>2</sub> fraction has to be changed according to the wanted application. This has to be done by a water gas shift reaction. To remember and for the use of our nomenclature:



The gases from biomass gasification have as impurities sulfur-, nitrogen- and chlorine compounds for example HCl. Therefore a catalyst would be very recommendable which is simple robust, cheap and not very sensitive towards these or part of these impurities. Catalysts on the basis of MoS<sub>2</sub> are candidates for these properties; [1] [2] [3] [4] [5]. This study deals with the reaction kinetics of the water gas shift reaction and the inverse reaction on those catalysts.

## 2 Experimental Design

### 2.1 The catalyst

The watergas shift reaction uses the gases CO and H<sub>2</sub>O, the inverse shift reaction the gases CO<sub>2</sub> and H<sub>2</sub>. The gases we employed had a purity of higher than 99.99%. Catalyst pellets consisting of Co-Mo-oxides on a Al<sub>2</sub>O<sub>3</sub>-matrix from the company Süd-Chemie (commercial product name: CoMo\_C49) were used. The characteristics of this catalyst are shown in table 1 on page 3.

Table 1: Physical-chemical properties of catalyst CoMo\_C49

<i>Chemical Composition</i>		<i>Physical Properties</i>	
CoO	3.5 mass-%	Shape	extruded
MoO <sub>3</sub>	10.0 mass-%	Size	2.5 - 3 mm
Al <sub>2</sub> O <sub>3</sub>	86 mass-%	Bulk density	0.6 kg/l
		Surface area	250 m <sup>2</sup> /g
		Pore volume	0.6 cm <sup>3</sup> /g

The oxidic form of the catalyst was activated with a gas mixture at 1 bar of H<sub>2</sub> and H<sub>2</sub>S. The concentration of H<sub>2</sub>S was 3000 – 3100 ppm. The amount

of H<sub>2</sub>S taken up by the catalyst was 57.4 mg-H<sub>2</sub>S/g-catalyst. The detailed instruction for sulfidation is shown in the appendix section 4.1 on page 37.

The activated catalyst CoMo\_C49 was analysed with a surface investigation equipment AutoChem 2910 from Micromeritics company. The obtained characteristics are shown in table 2 on page 4.

Table 2: Properties of the sulfidated catalyst CoMo\_C49. TPD is an abbreviation for temperature programmed desorption.  $E_d$  is the activation energy of desorption.

<i>Method</i>	<i>TPD</i> $E_d$ [kJ/mol]	<i>BET</i> (N <sub>2</sub> ) 1 Point-method
Surface area [m <sup>2</sup> /g-cat ]		179
Monolayer [cm <sup>3</sup> /g-cat ]		41
H <sub>2</sub> O	46	
CO <sub>2</sub>	33	
CO	23	
H <sub>2</sub>	0	

For the temperature programmed desorption (TPD) a kinetical desorption process of first order is assumed, shown in equation 1. After 60 minutes of adsorption of one of the respective gases, different temperature gradients for the desorption are started. The gas concentration peaks are recorded with a thermal conductivity detector and the peak maximum temperature was determined.

$$\frac{dc}{dt} = k(T(t))c \quad (1)$$

If for the temperature  $T(t)$  a linear gradient  $\beta$  in time  $t$  is used,  $T_0 + \beta t$ , equation 1 is transformed to equation 2. The symbol  $E_d$  is the activation energy of desorption and  $R$  is the universal gas constant.

$$\frac{dc}{dt} = k_0 \exp\left(\frac{-E_d}{R(T_0 + \beta t)}\right)c \quad (2)$$

The condition for the peak maximum temperature  $T_p$  is given by equation 3

$$\frac{d^2c}{dt^2} = 0 \quad (3)$$

From this condition and some algebraic rearrangements the following equation 4 results:

$$\log_{10}\left(\frac{T_p^2}{\beta}\right) = \frac{E_d}{2.303RT_p} + \log_{10}\left(\frac{E_d}{Rk_0}\right) \quad (4)$$

From equation 4 using the linear regression of  $\log_{10}\left(\frac{T_p^2}{\beta}\right)$  versus  $\frac{1}{T_p}$  gives a slope proportional to  $E_d$ .

## 2.2 The experimental fixed bed reactor

For the investigation of the shift- and inverse shift reactions on the sulfidic activated catalyst a reactor designed up to 30 bar is shown in figure 1 on page 6.

The apparatus consists of 4 parts:

1. five mass flow meters with control devices for the feed of the gases
2. a ceramic tube flow reactor manufactured of  $\text{Al}_2\text{O}_3$  surrounded by an electric heater; a removeable ceramic crucible which fits into the ceramic tub was used for holding 1.1 ml catalyst and 4 thermocouples
3. a control valve to obtain a constant pressure
4. a heatable gas pipe at atmospheric pressure with a mixing chamber which can be used to dilute the reaction gases with noble gases followed by two parallel arranged analytical devices (gas chromatography and mass spectroscopy).

The five mass flow and control devices (usable up to 64 bar) supplied with analogue electrical output were obtained from Wagner enterprises. Four of them were used to control the gas flow whereas the fifth equipped with an evaporation unit (CEM) (usable up to 200 °C) controlled the liquid (we used water) flow. The gas mass flow devices were calibrated with  $\text{N}_2$  to a maximum flow rate of 50  $\text{mln}/\text{min}$ . mln stands for ml at norm conditions which means 0 °C and 101325 Pa. The liquid mass flow controller calibrated with water had a flow range up to 5 g/h. All gas pipes installed after the mass flow controllers were connected to each other by stop-flow valves. Two resulting gas pipes were leading to the reactor whereof only the water vapor tube was heatable. An additional heatable gas pipe at atmospheric pressure to bypass the reactor was installed in order to analyse the feed gas mixture.

From Politec enterprises we obtained an  $\text{Al}_2\text{O}_3$  ceramic rod of 300 mm length and 25 mm diameter. A drilling hole with 115 mm length and 10 mm diameter was made from one side, from the other the drilling was different

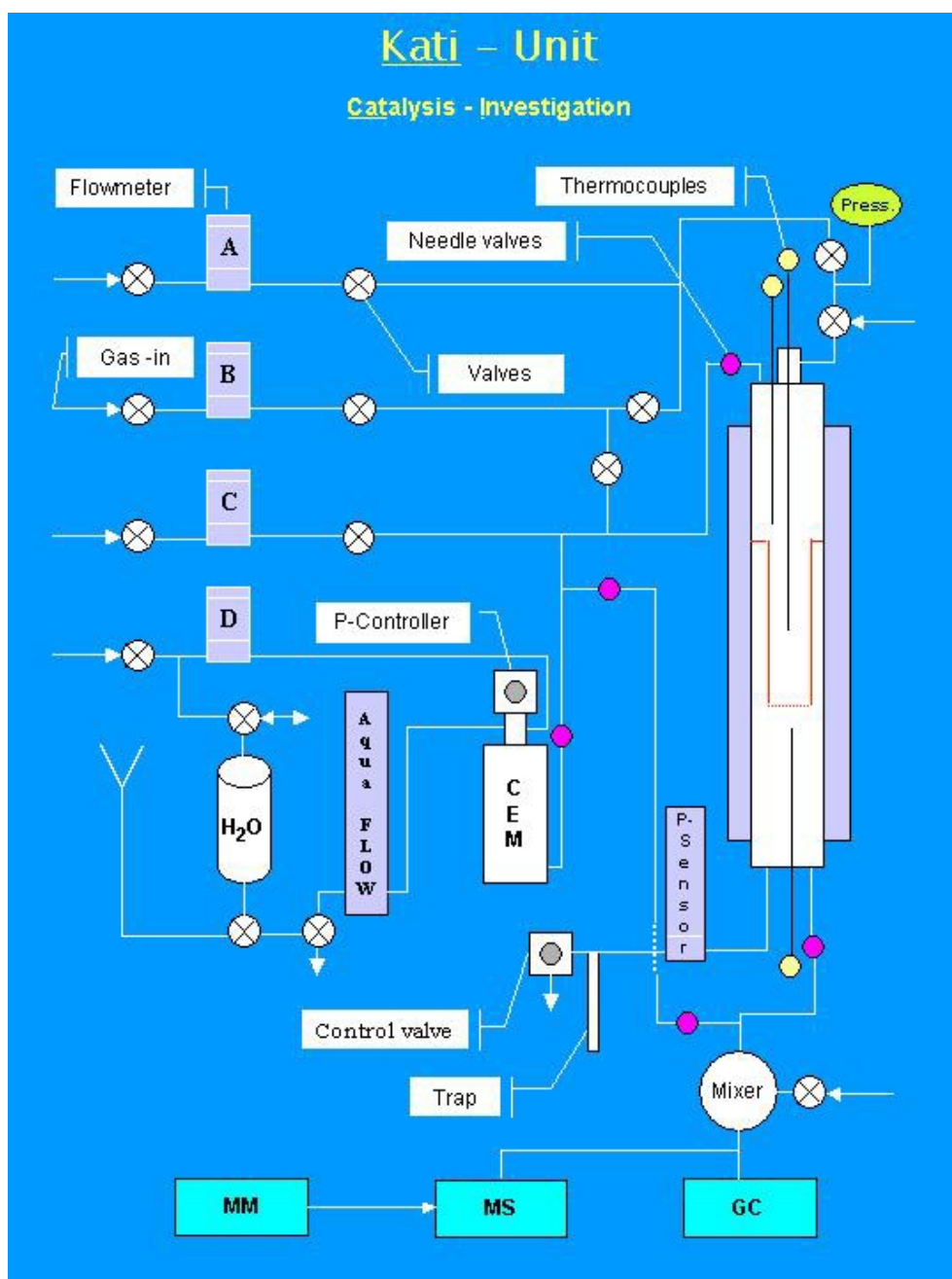


Figure 1: Fixed Bed Apparatus for Kinetic Measurements for Catalytic Reactions

with 185 mm length and 12 mm diameter. A crucible of length 35 mm and total volume of 1.51 ml was located in the resulting constriction. The leak



test was performed at 30 bar. The surface of the ceramic bar was worked on to get helical grooves. A heating wire (1 meter gauge Cantal wire) was wound up around these grooves. The electrical power of the resulting heating was about 180 W. The thermal isolation to the surrounding consisted of ceramic wool and high-grade steel sheet. High-grade metal cups containing O-rings were screwed on both ends of the tube reactor. Through these cups are leading the gas supply pipes and the gas outlet pipes and thermocouples.

The reactor outlet consists of two heatable gas lines. One line is leading to the pressure control valve connected to a pressure converter of Haenni enterprises usable up to 60 bar and 200 °C. The pressure control valve is usable only up to 70 °C, therefore a condenser with 20 ml volume was installed before the control valve in order to ensure an optimal functioning of this control unit. The other line is going via a needle valve to the gas mixing chamber and to the analytical devices.

The product gas were, depending on their composition, diluted with Ar in the mixing chamber. The dilute gases were leading simultaneously in heatable pipes to the analytic devices. The first device was a micro gas chromatograph G2890A of Agilent company with two columns (molecular sieve 5Å, 12 m x 0.32 mm; PoraPak Q, 8 m x 0.32 mm) and a thermal conductivity detector. The second analytic device was a quadrupole mass spectrometer of Pfeiffer company (Thermo Star 200) with 2 detectors (Faraday, CH-TRON) and a mass range up to 300 amu.

The micro gas chromatograph is working isothermal at 70 °C using an injection time of 20 ms. An analysis run was ended after 2 minutes. The gases He, H<sub>2</sub>, N<sub>2</sub>, O<sub>2</sub>, CH<sub>4</sub>, CO were detected at the end of the molecular sieve column; the gases Ar, CH<sub>4</sub>, CO<sub>2</sub>, H<sub>2</sub>S, H<sub>2</sub>O were detected after the PoraPlot column. Hydrocarbons like C<sub>2</sub>H<sub>4</sub>, C<sub>2</sub>H<sub>6</sub> and C<sub>3</sub>-components were not detected.

The catalytic reaction was observed online by mass spectrometry using different output methods like multiple ionization detection or multiple concentration detection or analog scan presentation. The data acquisition system of the Interlution company and home-built electronic and mechanical devices were used to record all the necessary parameter of the experimental setup to an Access data base.

### 2.3 Carrying out of the kinetic experiments

The reactor could be used up to maximum total flow rate of 200 ml<sup>h</sup>/min. Previous studies showed that below 250 °C only very minor conversions could be found. The experiments were performed at 3 temperatures 250 °C 300 °C 350 °C. The total pressure used was between 1 bar and 21 bar. The reactand

## Reaktion bei 4 bar

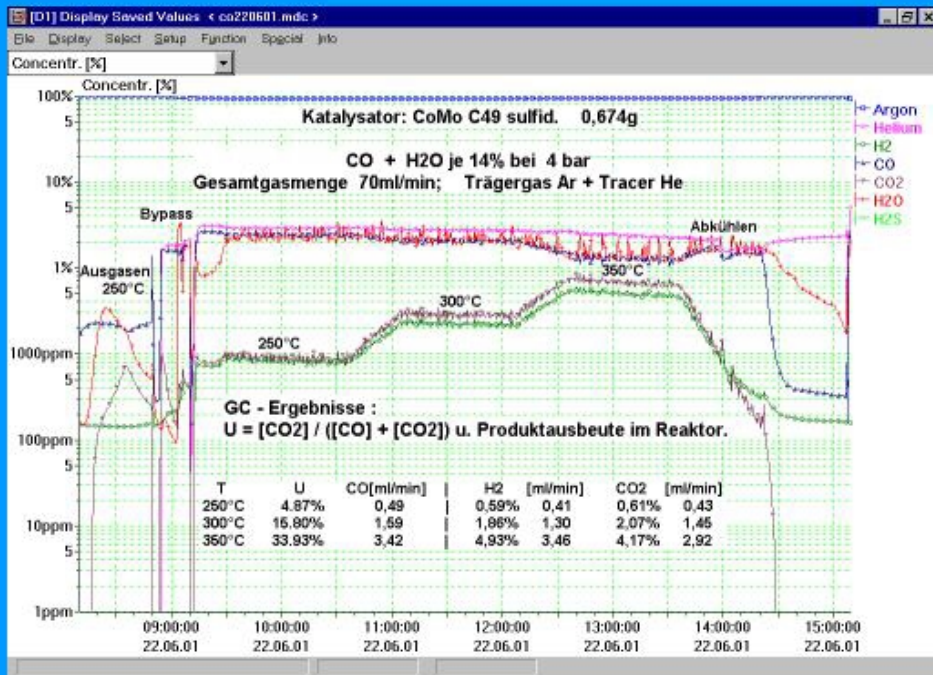


Figure 2: Example run with three different reaction temperatures

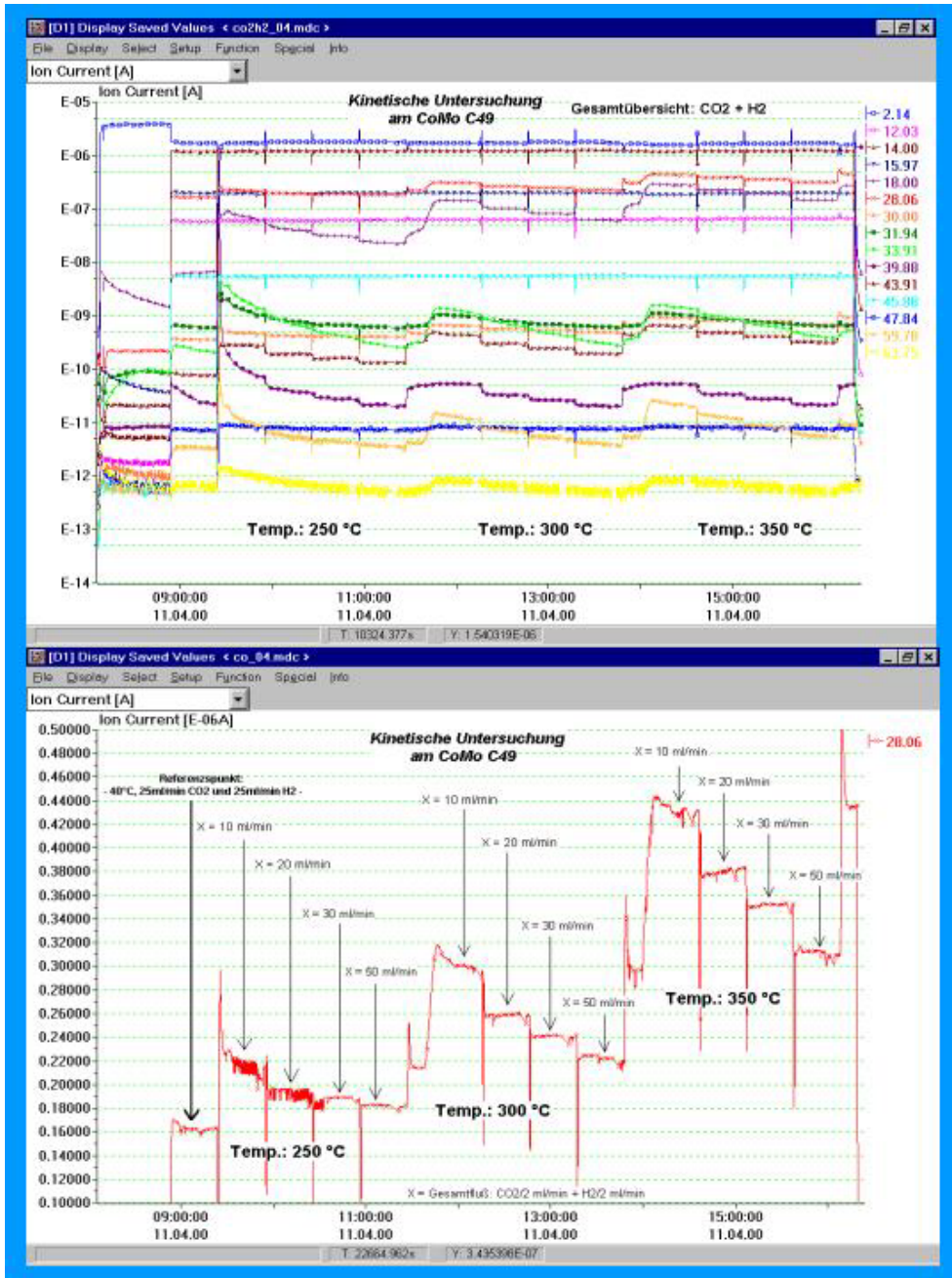
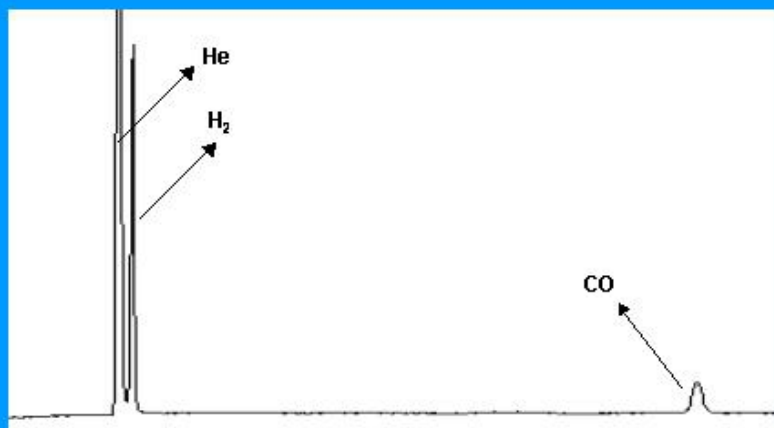


Figure 3: Example mass spectra of one run: a) online record of different masses; b) recording of mass 28

## Mikro - GC • Chromatogramme

Säule A (MS 5A 12m)



Säule B (PPQ 8m)

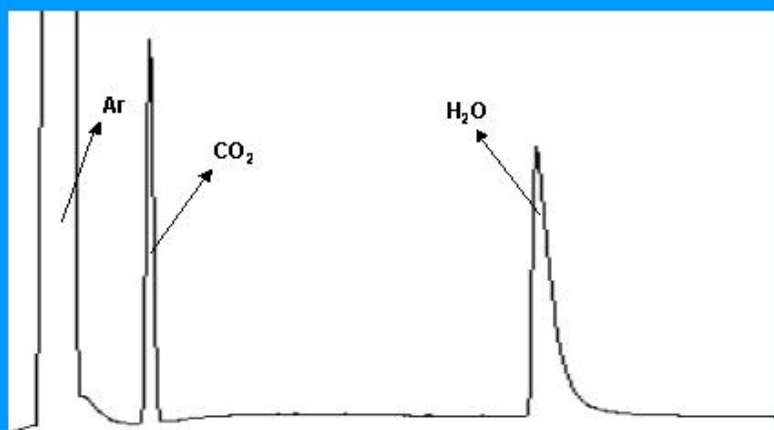


Figure 4: Example gaschromatographic analysis on both columns.

concentration in molar units was between 3.5% and 40%. The total flow was varied between 25 mln/min and 200 mln/min. Argon was used as the dilution gas and He was used as marker substance to get the absolute concentrations. The mixing ratio of the reaction gases varied from 1:1 to 1:4 and 4:1.

The weighed catalyst was put into the reactor, then all gas pipes were checked for leakages. A gas flow of 50 mln/min Ar was used to remove most of the absorbed water. This was done with a temperature program up to 350 °C until the content of water in the outlet was less than 1 ppm for more than 30 minutes.

After all parameters for the planned experiment (temperature, pressure, flow rates) had been adjusted, the experiment was executed until all the on-line measurements of the reaction gases with the mass spectrometer were constant. Then one or more gas chromatographic analysis were performed. After a successful quantitative analysis only one parameter was changed and the procedure was repeated.

In figure 2 on page 8 the online registration of an example run at three different temperatures at one constant pressure can be seen. In figure 3 on page 9 two different recordings of mass spectra are shown. The first one presents the ion currents (a measure for the concentrations) on a logarithmic scale of different masses during an experimental run. The other one shows the ion current of mass 28 on a linear scale during the experiment. In figure 4 on page 10 an example of the gaschromatographic analysis is shown.

## 3 Results and Discussions

### 3.1 Experimental results

In table 3 on page 12 the experimental results of all 266 experiments are shown. The horizontal lines are drawn for better reading. They were all made with the same catalyst and with one activation run. The symbols in the top and in the bottom lines characterizing the column entries are explained in the caption of table 3. For both the shift-reaction and the inverse-shift-reaction experiments at 3 temperatures (250 °C, 300 °C and 350 °C) were performed. The total pressures (composed of the educt feeds and noble gases Ar and He) were varied between 1 bar and 21 bar. The reaction time was a formal residual time calculated from the volume of the catalyst and the volume flow (at the respective temperature and pressure). More than half of the experiments were performed with equimolar educt feeds. The rest of the experiments used a feed ratio of 1:4 or 4:1. In three experiments no conversion was found (39, 56, 61) and they were therefore omitted in the table.

All the concentrations of CO, H<sub>2</sub>O, CO<sub>2</sub> and H<sub>2</sub> were determined by gas chromatography and simultaneously monitored with mass spectrometry. We used the feed concentrations, the stoichiometry and the concentrations of CO and CO<sub>2</sub> for the calculation of all the concentrations after the reaction, the measurements of the concentrations CO and CO<sub>2</sub> being more accurate than those measurements of the concentrations of H<sub>2</sub>O and H<sub>2</sub> and because there were no (relevant) minor products. These former mentioned concentrations and the feed concentrations are shown in table 3 in units mbar. The concentrations of H<sub>2</sub>O and H<sub>2</sub> were only used to check the experiments for consistency. Nearly all experiments have different initial feed flows (there are some repetitions) or different outer parameters like total pressure and temperature. Therefore it is impossible to display time-conversion plots (with all other parameters held constant) with more than two (initial and end concentration) or sometimes three experimental points.

Table 3: Summary table of all experimental results

- No* is the reference number of the experiment
- T* is the temperature in K
- p* is the total pressure in bar
- t* is the formal reaction time in seconds
- fco* is the feed concentration of CO in mbar
- fh2o* is the feed concentration of H<sub>2</sub>O in mbar
- fh2* is the feed concentration of H<sub>2</sub> in mbar
- fco2* is the feed concentration of CO<sub>2</sub> in mbar
- co* is the conc. of CO in mbar after the reaction
- h2o* is the conc. of H<sub>2</sub>O in mbar after the reaction
- h2* is the conc. of H<sub>2</sub> in mbar after the reaction
- co2* is the conc. of CO<sub>2</sub> in mbar after the reaction

No	T	p	t	fco	fh2o	fh2	fco2	co	co2	h2	h2o
1	523	5.0	2.42	717.7	772.5	0.0	0.0	693.5	24.3	24.3	748.2
2	573	5.0	2.22	719.3	766.8	0.0	0.0	633.6	85.7	85.7	681.1
3	623	5.0	2.04	721.4	756.1	0.0	0.0	473.0	248.4	248.4	507.7
4	523	1.0	0.17	35.0	35.4	0.0	0.0	34.6	0.4	0.4	35.0
5	523	5.0	0.84	174.5	175.2	0.0	0.0	171.2	3.3	3.3	171.8
6	573	5.0	0.77	174.7	177.0	0.0	0.0	163.8	10.9	10.9	166.1
7	623	5.0	0.70	174.4	178.3	0.0	0.0	140.7	33.7	33.7	144.6
8	623	1.0	0.14	34.9	36.6	0.0	0.0	30.9	4.0	4.0	32.7
9	523	1.0	0.34	70.7	68.6	0.0	0.0	69.7	1.0	1.0	67.6
10	523	5.0	1.70	356.6	372.3	0.0	0.0	347.9	8.7	8.7	363.7
11	573	5.0	1.55	353.2	365.6	0.0	0.0	323.8	29.4	29.4	336.2
12	623	5.0	1.42	351.8	371.2	0.0	0.0	266.0	85.8	85.8	285.4
13	623	1.0	0.28	70.2	73.9	0.0	0.0	60.1	10.2	10.2	63.7
14	523	1.0	0.67	139.7	147.2	0.0	0.0	137.4	2.4	2.4	144.8
15	523	5.0	3.38	701.9	731.6	0.0	0.0	676.4	25.5	25.5	706.1
No	T	p	t	fco	fh2o	fh2	fco2	co	co2	h2	h2o

No	T	p	t	fco	fh2o	fh2	fco2	co	co2	h2	h2o
16	573	5.0	3.08	700.8	733.1	0.0	0.0	619.1	81.7	81.7	651.3
17	623	5.0	2.83	699.4	726.4	0.0	0.0	478.1	221.3	221.3	505.2
18	623	1.0	0.57	140.4	146.3	0.0	0.0	116.3	24.1	24.1	122.3
19	523	1.0	0.23	47.0	48.9	0.0	0.0	46.5	0.5	0.5	48.4
20	523	5.0	1.13	236.2	244.5	0.0	0.0	232.0	4.3	4.3	240.2
21	573	5.0	1.03	235.9	248.5	0.0	0.0	221.6	14.3	14.3	234.2
22	623	5.0	0.95	235.8	245.3	0.0	0.0	191.4	44.4	44.4	200.9
23	623	1.0	0.19	47.2	48.9	0.0	0.0	42.2	5.0	5.0	43.8
24	523	1.0	1.33	276.4	288.1	0.0	0.0	270.2	6.2	6.2	281.9
25	523	5.0	6.67	1387.0	1443.1	0.0	0.0	1313.6	73.4	73.4	1369.7
26	573	5.0	6.09	1387.0	1443.1	0.0	0.0	1167.5	219.4	219.4	1223.7
27	623	5.0	5.66	1401.6	1412.3	0.0	0.0	823.0	578.6	578.6	833.6
28	623	1.0	1.11	274.9	292.1	0.0	0.0	218.5	56.4	56.4	235.7
29	523	1.0	0.68	0.0	0.0	398.4	400.1	3.3	396.7	395.0	3.3
30	523	5.0	3.40	0.0	0.0	1995.2	2005.3	30.9	1974.4	1964.3	30.9
31	573	5.0	3.12	0.0	0.0	2006.8	2018.2	103.5	1914.7	1903.3	103.5
32	623	5.0	2.85	0.0	0.0	1998.0	2005.1	245.9	1759.1	1752.1	245.9
33	623	1.0	0.57	0.0	0.0	398.2	399.9	34.1	365.9	364.1	34.1
34	523	1.0	1.36	0.0	0.0	321.2	319.5	3.4	316.1	317.8	3.4
35	523	5.0	6.80	0.0	0.0	1608.5	1604.3	27.7	1576.6	1580.7	27.7
36	573	5.0	6.20	0.0	0.0	1607.4	1603.2	98.7	1504.5	1508.7	98.7
37	623	5.0	5.71	0.0	0.0	1611.3	1604.6	225.7	1378.9	1385.6	225.7
38	623	1.0	1.14	0.0	0.0	321.1	319.9	32.8	287.1	288.3	32.8
40	523	5.0	1.70	0.0	0.0	999.1	1004.0	6.5	997.5	992.6	6.5
41	573	5.0	1.55	0.0	0.0	1000.5	1002.2	31.8	970.3	968.7	31.8
42	623	5.0	1.43	0.0	0.0	999.1	1003.3	90.4	912.9	908.6	90.4
43	623	1.0	0.28	0.0	0.0	199.2	199.7	11.4	188.3	187.8	11.4
44	623	1.0	0.57	0.0	0.0	397.2	401.8	25.7	376.1	371.5	25.7
45	623	3.0	1.71	0.0	0.0	1194.8	1206.6	110.5	1096.2	1084.4	110.5
46	623	5.0	2.85	0.0	0.0	1993.8	2012.8	205.0	1807.8	1788.8	205.0
47	623	6.0	3.40	0.0	0.0	2382.8	2408.1	257.6	2150.4	2125.2	257.6
48	623	7.0	3.99	0.0	0.0	2794.3	2819.7	314.0	2505.6	2480.3	314.0
49	623	8.0	4.54	0.0	0.0	3187.0	3219.2	374.5	2844.7	2812.6	374.5
50	623	8.5	4.84	0.0	0.0	3395.1	3423.7	428.1	2995.5	2967.0	428.1
51	523	1.0	0.34	0.0	0.0	198.3	200.8	1.0	199.8	197.3	1.0
52	523	8.0	2.72	0.0	0.0	1595.9	1614.2	13.1	1601.1	1582.8	13.1
53	573	8.0	2.49	0.0	0.0	1593.0	1605.3	55.4	1549.9	1537.6	55.4
54	623	8.0	2.28	0.0	0.0	1591.4	1612.1	137.7	1474.3	1453.7	137.7
55	623	1.0	0.28	0.0	0.0	198.5	200.8	6.9	193.9	191.6	6.9
57	523	5.0	1.14	0.0	0.0	666.8	672.1	5.0	667.0	661.8	5.0
58	573	5.0	1.04	0.0	0.0	666.6	671.2	16.0	655.2	650.6	16.0
59	623	5.0	0.95	0.0	0.0	667.6	671.4	45.9	625.5	621.7	45.9
60	623	1.0	0.19	0.0	0.0	133.0	133.9	5.2	128.6	127.8	5.2
62	523	1.0	0.23	0.0	0.0	132.9	134.3	0.3	134.0	132.6	0.3
63	523	8.0	1.82	0.0	0.0	1066.7	1077.8	7.4	1070.4	1059.3	7.4
64	573	8.0	1.66	0.0	0.0	1068.0	1077.9	30.4	1047.5	1037.5	30.4
65	623	8.0	1.52	0.0	0.0	1064.7	1076.3	84.1	992.2	980.6	84.1
66	623	1.0	0.19	0.0	0.0	132.9	134.2	5.5	128.7	127.4	5.5
67	523	1.0	0.68	0.0	0.0	397.3	401.3	2.1	399.2	395.3	2.1
68	523	8.0	5.44	0.0	0.0	3195.6	3220.2	36.8	3183.4	3158.9	36.8
69	573	8.0	4.96	0.0	0.0	3191.6	3239.9	141.0	3098.9	3050.7	141.0
70	623	8.0	4.57	0.0	0.0	3199.8	3216.0	362.3	2853.8	2837.5	362.3
71	623	1.0	0.57	0.0	0.0	397.3	401.7	24.4	377.4	372.9	24.4
72	523	1.0	0.17	0.0	0.0	179.5	182.0	0.5	181.5	179.0	0.5
73	523	8.0	1.35	0.0	0.0	1438.9	1458.0	8.7	1449.3	1430.2	8.7
No	T	p	t	fco	fh2o	fh2	fco2	co	co2	h2	h2o

No	T	p	t	fco	fh2o	fh2	fco2	co	co2	h2	h2o
74	573	8.0	1.23	0.0	0.0	1440.7	1462.6	30.8	1431.8	1409.9	30.8
75	623	8.0	1.14	0.0	0.0	1438.9	1459.0	89.1	1369.9	1349.7	89.1
76	623	1.0	0.14	0.0	0.0	179.6	182.0	5.4	176.7	174.2	5.4
77	623	1.0	0.28	71.5	72.6	0.0	0.0	61.9	9.6	9.6	62.9
78	623	3.0	0.85	213.8	212.4	0.0	0.0	175.3	38.5	38.5	173.9
79	623	5.0	1.42	359.3	358.2	0.0	0.0	283.1	76.2	76.2	282.0
80	623	6.0	1.70	429.0	425.4	0.0	0.0	334.1	94.9	94.9	330.4
81	623	7.0	1.99	501.1	509.4	0.0	0.0	385.4	115.6	115.6	393.8
82	623	8.0	2.28	572.8	574.0	0.0	0.0	432.8	139.9	139.9	434.1
83	523	1.0	0.34	71.5	72.9	0.0	0.0	70.6	0.8	0.8	72.1
84	523	8.0	2.72	573.6	580.0	0.0	0.0	555.2	18.4	18.4	561.6
85	573	8.0	2.48	573.0	577.3	0.0	0.0	517.1	55.9	55.9	521.4
86	623	8.0	2.28	573.1	585.7	0.0	0.0	426.1	147.0	147.0	438.7
87	623	1.0	0.28	71.5	72.6	0.0	0.0	62.5	9.0	9.0	63.7
88	523	1.0	0.23	47.9	48.9	0.0	0.0	47.4	0.5	0.5	48.4
89	523	8.0	1.83	386.1	389.7	0.0	0.0	376.4	9.7	9.7	380.0
90	573	8.0	1.66	384.8	390.5	0.0	0.0	354.8	30.0	30.0	360.5
91	623	8.0	1.53	385.0	387.9	0.0	0.0	303.2	81.8	81.8	306.1
92	623	1.0	0.19	48.1	48.0	0.0	0.0	42.7	5.4	5.4	42.5
93	523	1.0	0.17	35.8	35.9	0.0	0.0	35.6	0.3	0.3	35.6
94	523	8.0	1.36	287.3	290.0	0.0	0.0	281.9	5.4	5.4	284.6
95	573	8.0	1.25	288.2	289.3	0.0	0.0	272.2	16.0	16.0	273.3
96	623	8.0	1.14	287.4	285.0	0.0	0.0	238.9	48.5	48.5	236.5
97	623	1.0	0.14	35.8	36.4	0.0	0.0	32.7	3.2	3.2	33.3
98	523	1.0	0.67	142.0	144.8	0.0	0.0	139.5	2.4	2.4	142.4
99	523	8.0	5.42	1142.7	1134.9	0.0	0.0	1092.9	49.8	49.8	1085.0
100	573	8.0	4.94	1143.6	1150.3	0.0	0.0	975.4	168.2	168.2	982.1
101	623	8.0	4.54	1145.8	1146.5	0.0	0.0	720.7	425.2	425.2	721.3
102	623	1.0	0.56	141.8	144.9	0.0	0.0	117.1	24.7	24.7	120.2
103	623	1.0	0.29	0.0	0.0	200.8	202.3	10.5	191.8	190.4	10.5
104	623	5.0	1.44	0.0	0.0	1006.4	1015.6	86.2	929.4	920.2	86.2
105	623	9.0	2.58	0.0	0.0	1806.7	1820.1	185.6	1634.5	1621.1	185.6
106	623	13.0	3.73	0.0	0.0	2607.5	2630.1	305.5	2324.7	2302.0	305.5
107	623	17.0	4.91	0.0	0.0	3433.4	3408.6	449.5	2959.0	2983.9	449.5
108	623	21.0	6.03	0.0	0.0	4216.3	4241.2	625.0	3616.2	3591.3	625.0
109	523	13.0	4.46	0.0	0.0	2617.3	2634.4	28.3	2606.1	2589.0	28.3
110	523	17.0	5.82	0.0	0.0	3417.2	3440.5	42.4	3398.1	3374.8	42.4
111	523	21.0	7.19	0.0	0.0	4221.8	4251.3	60.8	4190.4	4161.0	60.8
112	573	21.0	6.57	0.0	0.0	4231.8	4256.1	249.3	4006.7	3982.5	249.3
113	573	17.0	5.32	0.0	0.0	3423.9	3443.6	171.0	3272.6	3252.9	171.0
114	573	13.0	4.06	0.0	0.0	2610.9	2628.9	110.0	2518.8	2500.9	110.0
115	523	13.0	2.94	0.0	0.0	1709.7	1740.0	15.1	1724.9	1694.6	15.1
116	523	17.0	3.84	0.0	0.0	2234.7	2306.2	21.7	2284.6	2213.1	21.7
117	523	21.0	4.76	0.0	0.0	2766.1	2812.8	30.1	2782.7	2735.9	30.1
118	573	21.0	4.34	0.0	0.0	2767.7	2814.0	129.0	2684.9	2638.7	129.0
119	573	17.0	3.51	0.0	0.0	2236.9	2278.5	92.1	2186.4	2144.8	92.1
120	573	13.0	2.67	0.0	0.0	1705.6	1783.9	62.5	1721.4	1643.0	62.5
121	623	13.0	2.47	0.0	0.0	1709.8	1740.9	174.4	1566.5	1535.5	174.4
122	623	17.0	3.21	0.0	0.0	2231.0	2350.0	257.8	2092.2	1973.2	257.8
123	623	21.0	4.00	0.0	0.0	2770.3	2814.0	336.7	2477.4	2433.6	336.7
124	523	13.0	2.21	0.0	0.0	2310.3	2372.8	14.8	2358.0	2295.4	14.8
125	523	17.0	2.90	0.0	0.0	3031.7	3077.3	20.3	3057.0	3011.4	20.3
126	523	21.0	3.57	0.0	0.0	3730.9	3835.3	27.2	3808.1	3703.7	27.2
127	573	21.0	3.26	0.0	0.0	3728.2	3829.1	123.9	3705.2	3604.2	123.9
128	573	17.0	2.64	0.0	0.0	3024.1	3087.1	87.6	2999.5	2936.4	87.6
No	T	p	t	fco	fh2o	fh2	fco2	co	co2	h2	h2o



No	T	p	t	fco	fh2o	fh2	fco2	co	co2	h2	h2o
129	573	13.0	2.01	0.0	0.0	2299.6	2407.8	60.3	2347.5	2239.3	60.3
130	623	13.0	1.85	0.0	0.0	2304.4	2387.5	173.6	2213.9	2130.9	173.6
131	623	17.0	2.43	0.0	0.0	3026.1	3098.6	236.3	2862.3	2789.8	236.3
132	623	21.0	3.01	0.0	0.0	3745.8	3772.8	310.6	3462.2	3435.3	310.6
133	523	13.0	2.95	622.9	617.6	0.0	0.0	592.1	30.8	30.8	586.8
134	523	17.0	3.86	815.0	803.5	0.0	0.0	769.0	45.9	45.9	757.6
135	523	21.0	4.77	1009.3	999.0	0.0	0.0	950.7	58.6	58.6	940.4
136	573	21.0	4.35	1008.1	995.8	0.0	0.0	843.8	164.3	164.3	831.6
137	573	17.0	3.53	817.7	809.3	0.0	0.0	707.9	109.8	109.8	699.6
138	573	13.0	2.69	621.8	623.2	0.0	0.0	546.2	75.6	75.6	547.6
139	623	13.0	2.47	624.0	615.4	0.0	0.0	432.4	191.6	191.6	423.8
140	623	17.0	3.23	814.1	804.2	0.0	0.0	554.4	259.7	259.7	544.5
141	623	21.0	4.00	1006.7	1005.4	0.0	0.0	673.0	333.7	333.7	671.7
142	523	13.0	4.44	940.4	930.8	0.0	0.0	897.9	42.5	42.5	888.3
143	523	17.0	5.81	1228.2	1208.8	0.0	0.0	1160.0	68.2	68.2	1140.6
144	523	21.0	7.18	1512.1	1493.4	0.0	0.0	1417.8	94.4	94.4	1399.0
145	573	21.0	6.53	1510.6	1511.1	0.0	0.0	1213.1	297.5	297.5	1213.6
146	573	17.0	5.29	1226.0	1233.2	0.0	0.0	1015.1	211.0	211.0	1022.2
147	573	13.0	4.00	925.8	927.9	0.0	0.0	784.5	141.3	141.3	786.6
148	623	13.0	3.79	957.0	947.2	0.0	0.0	583.7	373.3	373.3	573.9
149	623	17.0	4.90	1232.2	1237.1	0.0	0.0	730.5	501.8	501.8	735.3
150	623	21.0	6.02	1511.9	1501.5	0.0	0.0	912.5	599.4	599.4	902.1
151	523	13.0	2.27	479.4	479.6	0.0	0.0	465.0	14.4	14.4	465.1
152	523	17.0	2.88	612.4	612.8	0.0	0.0	592.4	20.0	20.0	592.9
153	523	21.0	3.57	754.1	742.3	0.0	0.0	719.8	34.3	34.3	707.9
154	573	21.0	3.26	754.8	748.3	0.0	0.0	666.6	88.2	88.2	660.2
155	573	17.0	2.64	611.7	603.2	0.0	0.0	549.9	61.8	61.8	541.5
156	573	13.0	2.04	470.7	470.9	0.0	0.0	428.3	42.4	42.4	428.5
157	623	13.0	1.85	467.2	467.5	0.0	0.0	359.4	107.9	107.9	359.6
158	623	17.0	2.43	611.6	609.7	0.0	0.0	453.4	158.2	158.2	451.5
159	623	21.0	2.99	752.1	752.3	0.0	0.0	517.7	234.4	234.4	518.0
160	523	13.0	7.35	1124.5	1093.2	0.0	0.0	1051.8	72.7	72.7	1020.5
161	523	17.0	9.61	1459.4	1428.8	0.0	0.0	1340.1	119.2	119.2	1309.6
162	523	21.1	11.87	1807.6	1801.6	0.0	0.0	1654.2	153.4	153.4	1648.2
163	573	21.0	10.84	1799.1	1765.6	0.0	0.0	1308.8	490.3	490.3	1275.3
164	573	17.0	8.74	1458.4	1453.6	0.0	0.0	1059.3	399.1	399.1	1054.5
165	573	13.0	6.72	1120.7	1111.5	0.0	0.0	873.3	247.4	247.4	864.1
166	623	13.0	6.18	1118.3	1089.3	0.0	0.0	565.8	552.5	552.5	536.8
167	623	17.0	8.07	1459.8	1414.6	0.0	0.0	754.1	705.7	705.7	709.0
168	623	21.0	9.96	1801.9	1791.3	0.0	0.0	907.4	894.5	894.5	896.7
169	523	13.0	8.85	0.0	0.0	5154.0	5243.9	72.3	5171.6	5081.7	72.3
170	523	17.0	11.61	0.0	0.0	6747.3	6835.9	117.2	6718.7	6630.1	117.2
171	523	21.0	14.35	0.0	0.0	8329.8	8478.8	178.5	8300.3	8151.3	178.5
172	573	21.0	13.07	0.0	0.0	8332.0	8468.9	715.8	7753.2	7616.2	715.8
173	573	17.0	10.60	0.0	0.0	6752.1	6850.7	470.0	6380.6	6282.0	470.0
174	573	13.0	8.08	0.0	0.0	5149.8	5260.3	302.7	4957.6	4847.1	302.7
175	623	13.0	7.31	0.0	0.0	5058.9	5394.0	797.8	4596.3	4261.1	797.8
176	623	17.1	9.75	0.0	0.0	6757.8	6867.6	1171.3	5696.3	5586.5	1171.3
177	623	21.0	12.04	0.0	0.0	8324.1	8473.0	1966.5	6506.5	6357.6	1966.5
178	523	13.0	8.83	0.0	0.0	1964.8	1954.1	31.8	1922.3	1933.0	31.8
179	523	17.0	11.44	0.0	0.0	2539.1	2687.9	50.9	2637.0	2488.2	50.9
180	523	21.0	14.18	0.0	0.0	3159.6	3201.6	65.3	3136.3	3094.3	65.3
181	573	21.0	12.92	0.0	0.0	3152.3	3307.4	252.4	3055.0	2900.0	252.4
182	573	17.0	10.49	0.0	0.0	2555.0	2605.4	181.0	2424.4	2374.0	181.0
183	573	13.0	7.95	0.0	0.0	1933.7	2114.4	131.3	1983.1	1802.4	131.3
No	T	p	t	fco	fh2o	fh2	fco2	co	co2	h2	h2o

No	T	p	t	fco	fh2o	fh2	fco2	co	co2	h2	h2o
184	623	13.0	7.42	0.0	0.0	1961.5	1968.1	274.8	1693.3	1686.6	274.8
185	623	17.0	9.67	0.0	0.0	2560.9	2583.8	378.4	2205.4	2182.5	378.4
186	623	21.0	11.99	0.0	0.0	3170.6	3185.2	490.2	2695.0	2680.4	490.2
187	523	13.0	8.78	0.0	0.0	1951.0	1983.8	49.2	1934.7	1901.9	49.2
188	523	17.0	11.52	0.0	0.0	2560.1	2603.1	72.2	2531.0	2487.9	72.2
189	523	21.1	14.23	0.0	0.0	3174.1	3228.2	95.6	3132.7	3078.5	95.6
190	573	21.0	12.97	0.0	0.0	3153.8	3212.1	290.5	2921.6	2863.3	290.5
191	573	17.0	10.48	0.0	0.0	2551.7	2603.8	215.2	2388.5	2336.4	215.2
192	573	13.0	8.02	0.0	0.0	1950.8	1993.8	149.8	1844.1	1801.0	149.8
193	623	13.0	7.36	0.0	0.0	1948.5	1986.0	314.2	1671.8	1634.3	314.2
194	623	17.0	9.64	0.0	0.0	2551.3	2594.2	418.9	2175.3	2132.4	418.9
195	623	21.0	11.91	0.0	0.0	3148.4	3206.6	529.0	2677.6	2619.4	529.0
196	523	1.0	0.23	0.0	0.0	53.3	213.5	0.4	213.1	52.8	0.4
197	523	11.0	2.50	0.0	0.0	587.2	2352.0	10.6	2341.3	576.5	10.6
198	523	21.0	4.78	0.0	0.0	1123.0	4495.7	25.7	4470.0	1097.3	25.7
199	573	21.0	4.36	0.0	0.0	1121.8	4486.0	102.4	4383.7	1019.5	102.4
200	573	11.0	2.28	0.0	0.0	587.3	2354.6	41.7	2312.9	545.7	41.7
201	573	1.0	0.21	0.0	0.0	53.1	213.7	1.6	212.0	51.5	1.6
202	623	1.0	0.19	0.0	0.0	53.2	213.5	5.3	208.2	48.0	5.3
203	623	11.0	2.10	0.0	0.0	587.6	2353.8	117.7	2236.1	469.9	117.7
204	623	21.0	4.00	0.0	0.0	1125.2	4486.3	268.4	4217.9	856.8	268.4
205	523	1.0	0.45	0.0	0.0	50.2	200.1	1.0	199.1	49.2	1.0
206	523	11.0	5.00	0.0	0.0	551.8	2202.7	17.5	2185.3	534.3	17.5
207	523	21.0	9.53	0.0	0.0	1056.0	4204.0	40.7	4163.3	1015.3	40.7
208	573	21.0	8.68	0.0	0.0	1053.8	4205.4	152.9	4052.4	900.9	152.9
209	573	11.0	4.56	0.0	0.0	553.7	2192.3	58.5	2133.9	495.2	58.5
210	573	1.0	0.41	0.0	0.0	50.1	199.0	2.5	196.5	47.6	2.5
211	623	1.0	0.38	0.0	0.0	50.4	199.9	8.0	191.9	42.4	8.0
212	623	11.0	4.19	0.0	0.0	553.1	2201.9	149.6	2052.3	403.5	149.6
213	623	21.0	8.01	0.0	0.0	1057.1	4195.8	327.1	3868.7	730.0	327.1
214	523	1.0	0.45	0.0	0.0	199.7	49.8	0.8	49.0	199.0	0.8
215	523	11.0	4.99	0.0	0.0	2200.7	550.6	14.3	536.3	2186.4	14.3
216	523	21.0	9.56	0.0	0.0	4192.6	1054.2	39.5	1014.7	4153.1	39.5
217	573	21.0	8.73	0.0	0.0	4195.5	1054.9	130.5	924.4	4065.0	130.5
218	573	11.0	4.56	0.0	0.0	2200.7	551.1	54.5	496.6	2146.2	54.5
219	573	1.0	0.41	0.0	0.0	199.7	50.0	2.4	47.6	197.3	2.4
220	623	1.0	0.38	0.0	0.0	199.6	49.8	6.7	43.2	193.0	6.7
221	623	11.0	4.20	0.0	0.0	2208.1	548.4	127.8	420.6	2080.2	127.8
222	623	21.0	7.98	0.0	0.0	4214.3	1048.3	285.2	763.1	3929.0	285.2
223	523	1.0	0.23	0.0	0.0	200.0	50.0	0.3	49.7	199.7	0.3
224	523	11.0	2.50	0.0	0.0	2206.7	550.5	9.5	541.0	2197.2	9.5
225	523	21.0	4.77	0.0	0.0	4208.8	1049.5	22.1	1027.4	4186.7	22.1
226	573	21.0	4.38	0.0	0.0	4234.5	1059.3	89.2	970.1	4145.2	89.2
227	573	11.0	2.28	0.0	0.0	2205.8	550.7	35.6	515.1	2170.2	35.6
228	573	1.0	0.21	0.0	0.0	200.1	50.0	1.7	48.3	198.4	1.7
229	623	1.0	0.19	0.0	0.0	199.9	50.0	4.9	45.1	195.1	4.9
230	623	11.0	2.10	0.0	0.0	2206.3	550.6	92.0	458.6	2114.3	92.0
231	623	21.0	4.00	0.0	0.0	4205.2	1049.8	218.5	831.4	3986.7	218.5
232	523	1.0	0.23	199.7	50.4	0.0	0.0	199.0	0.7	0.7	49.7
233	523	11.0	2.50	2206.4	546.4	0.0	0.0	2170.8	35.6	35.6	510.8
234	523	21.0	4.77	4207.2	1046.7	0.0	0.0	4113.5	93.7	93.7	953.0
235	573	21.0	4.34	4199.9	1051.7	0.0	0.0	3891.1	308.8	308.8	742.9
236	573	11.0	2.28	2203.2	549.8	0.0	0.0	2120.1	83.1	83.1	466.8
237	573	1.0	0.21	199.9	50.4	0.0	0.0	196.8	3.1	3.1	47.3
238	623	1.0	0.19	200.0	49.9	0.0	0.0	188.3	11.7	11.7	38.2
No	T	p	t	fco	fh2o	fh2	fco2	co	co2	h2	h2o

No	T	p	t	fco	fh2o	fh2	fco2	co	co2	h2	h2o
239	623	11.0	2.10	2207.4	530.2	0.0	0.0	2000.7	206.7	206.7	323.5
240	623	21.0	4.00	4202.4	1066.8	0.0	0.0	3632.9	569.4	569.4	497.4
241	523	1.0	0.45	265.3	70.5	0.0	0.0	264.0	1.4	1.4	69.1
242	523	11.0	4.98	2925.2	786.4	0.0	0.0	2877.1	48.2	48.2	738.2
243	523	21.0	9.49	5584.3	1476.8	0.0	0.0	5426.1	158.2	158.2	1318.7
244	573	21.0	8.68	5595.1	1442.6	0.0	0.0	5015.0	580.2	580.2	862.5
245	573	11.0	4.55	2929.9	756.8	0.0	0.0	2720.8	209.2	209.2	547.7
246	573	1.0	0.41	264.4	74.4	0.0	0.0	258.3	6.1	6.1	68.3
247	523	1.0	0.45	265.7	69.0	0.0	0.0	264.5	1.2	1.2	67.8
248	523	11.0	4.99	2933.0	738.6	0.0	0.0	2885.6	47.3	47.3	691.3
249	523	21.0	9.52	5588.2	1437.2	0.0	0.0	5414.1	174.1	174.1	1263.0
250	623	21.0	8.00	5595.9	1410.2	0.0	0.0	4457.1	1138.8	1138.8	271.4
251	623	21.0	7.98	5594.4	1435.2	0.0	0.0	4570.9	1023.5	1023.5	411.7
252	623	1.0	0.38	266.5	68.0	0.0	0.0	251.7	14.9	14.9	53.1
253	623	11.0	4.18	2937.8	749.0	0.0	0.0	2566.0	371.8	371.8	377.2
254	623	11.0	4.19	2942.2	731.1	0.0	0.0	2576.3	365.9	365.9	365.2
255	623	21.0	7.79	5480.0	1401.6	0.0	0.0	4680.7	799.3	799.3	602.3
256	623	21.0	7.99	5608.5	1408.1	0.0	0.0	4679.3	929.1	929.1	479.0
257	623	21.0	7.97	5604.5	1434.3	0.0	0.0	4688.9	915.6	915.6	518.7
258	523	1.0	0.45	39.7	162.7	0.0	0.0	38.8	0.9	0.9	161.8
259	523	1.0	0.23	20.1	81.4	0.0	0.0	19.8	0.3	0.3	81.0
260	523	11.0	2.49	221.2	885.6	0.0	0.0	210.7	10.4	10.4	875.1
261	523	21.0	4.75	421.1	1714.4	0.0	0.0	386.1	35.0	35.0	1679.4
262	573	21.0	4.34	417.6	1717.8	0.0	0.0	309.1	108.5	108.5	1609.3
263	573	11.0	2.28	222.1	902.4	0.0	0.0	181.5	40.6	40.6	861.8
264	573	1.0	0.21	20.1	85.5	0.0	0.0	18.8	1.3	1.3	84.2
265	623	1.0	0.19	20.3	82.0	0.0	0.0	15.9	4.3	4.3	77.7
266	623	11.0	2.10	222.4	854.4	0.0	0.0	131.8	90.6	90.6	763.8
267	623	21.0	4.00	422.6	1702.5	0.0	0.0	192.9	229.7	229.7	1472.7
268	623	11.0	2.10	222.2	893.4	0.0	0.0	127.7	94.4	94.4	798.9
269	623	1.0	0.19	20.2	80.7	0.0	0.0	16.6	3.6	3.6	77.1
No	T	p	t	fco	fh2o	fh2	fco2	co	co2	h2	h2o

### 3.2 Experimental results with equimolar feed concentrations

Considering only the experiments with equimolar feed concentrations and from those only these not near the equilibrium a simple kinetical model can be applied as a first guess. This can be done because the simple stoichiometry with high experimental selectivity causes the both reactands and both the reaction products to have the same concentration at any reaction time. The symbol  $c(t)$  in the equations is used for the concentration of the reactands.

$$\frac{dc(t)}{dt} = -k \cdot c(t)^n \quad \text{with initial condition} \quad c(0) = c_0 \quad (5)$$

The solution of differential equation 5 is the following expression:

$$c(t) = \left( \frac{n \left(\frac{1}{c_0}\right)^{n-1}}{n-1} - \frac{\left(\frac{1}{c_0}\right)^{n-1}}{n-1} - kt + knt \right)^{\frac{1}{1-n}} \quad (6)$$

The solution shown in equation 6 is not suitable for graphical applications. It is rearranged to form equation 7 .

$$t = -\frac{\left(\frac{1}{c_0}\right)^{n-1} - \left(\frac{1}{c(t)}\right)^{n-1}}{k(n-1)} \quad (7)$$

The exponent  $n$  has to be assumed or guessed. Then the experimental points can be plotted as  $\left(\frac{1}{c_0}\right)^{n-1} - \left(\frac{1}{c(t)}\right)^{n-1}$  versus reaction time  $t$  and should result in a straight line.

Assuming for the exponent  $n = \frac{1}{2}$ , the experimental results can be seen in figure 5 on page 18 to figure 10 on page 19. In these figures the vertical axis is used for  $\sqrt{c_0} - \sqrt{c}$ , where  $c$  stands for the concentrations in mbar of CO or H<sub>2</sub>O in the watergas shift reaction and for the concentration in mbar of CO<sub>2</sub> or H<sub>2</sub> in the inverse shift reaction . The bubble size in the plots is proportional to the total pressure of the experiment. For each temperature (250 °C, 300 °C and 350 °C ) a separate figure is shown. The slope of the straight line which can be drawn through the experimental points is a measure for the reaction rate constant  $k$  for the assumed kinetics  $\frac{dc}{dt} = -kc^{0.5}$ .

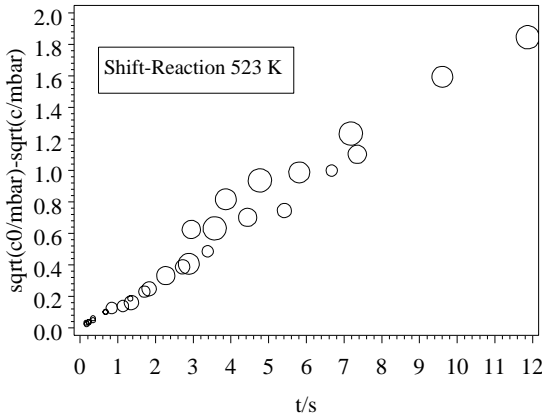


Figure 5: Equimolar reactands (CO and H<sub>2</sub>O)  $\sqrt{c_0} - \sqrt{c}$  versus reaction time at 523 K in the watergas shift reaction

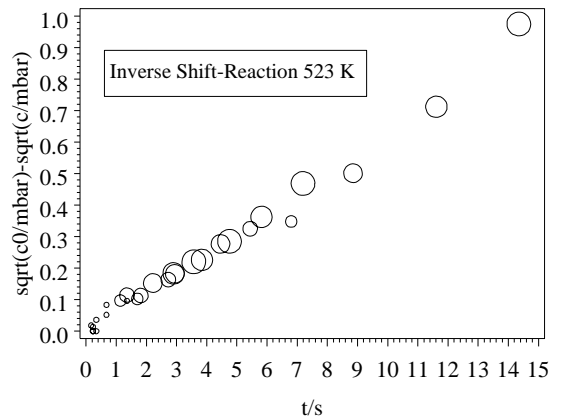


Figure 6: Equimolar reactands (CO<sub>2</sub> and H<sub>2</sub>)  $\sqrt{c_0} - \sqrt{c}$  versus reaction time at 523 K in the inverse shift reaction

If the exponent  $n$  is not fixed, the more general equation (6) has to be used for a nonlinear regression with the same experimental data. To get an equation for all temperatures, the parameter  $k$  has to be substituted by an Arrhenius expression.

$$c(t) = \left( \frac{n \left(\frac{1}{c_0}\right)^{n-1}}{n-1} - \frac{\left(\frac{1}{c_0}\right)^{n-1}}{n-1} + k_0 e^{-\frac{E_a}{RT}} (nt - t) \right)^{\frac{1}{1-n}} \quad (8)$$

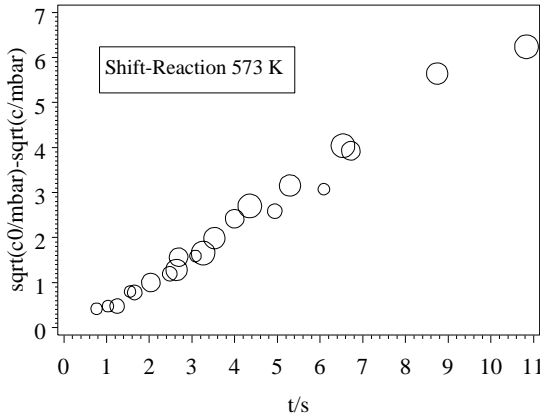


Figure 7: Equimolar reactands (CO and H<sub>2</sub>O)  $\sqrt{c_0} - \sqrt{c}$  versus reaction time at 573 K in the watergas shift reaction

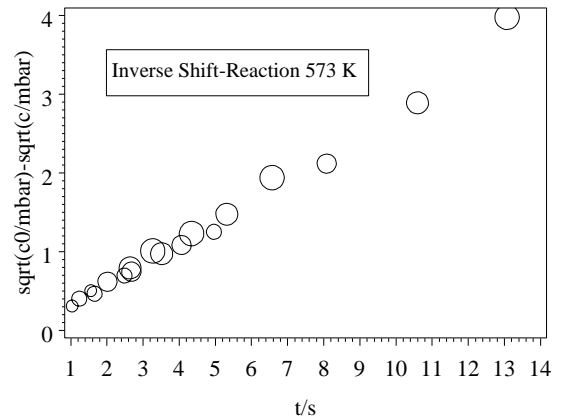


Figure 8: Equimolar reactands (CO<sub>2</sub> and H<sub>2</sub>)  $\sqrt{c_0} - \sqrt{c}$  versus reaction time at 573 K in the inverse shift reaction

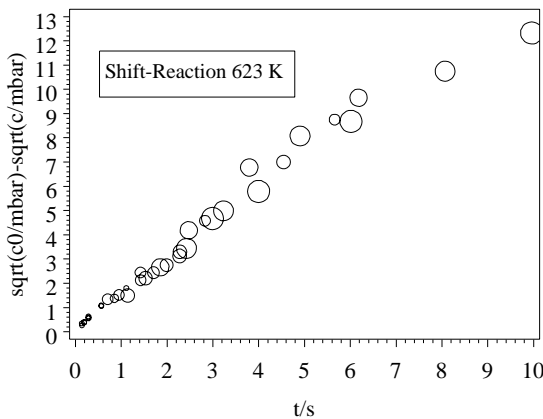


Figure 9: Equimolar reactands (CO and H<sub>2</sub>O)  $\sqrt{c_0} - \sqrt{c}$  versus reaction time at 623 K in the watergas shift reaction

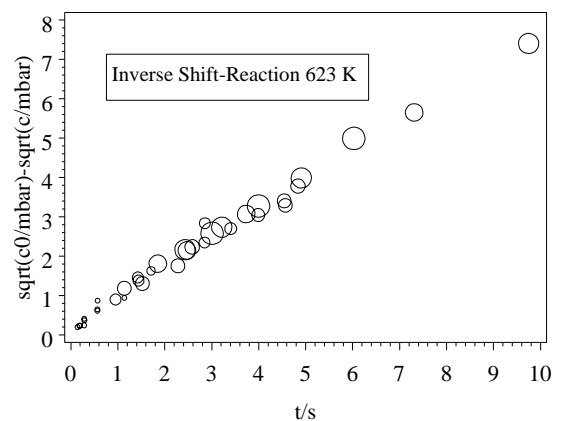


Figure 10: Equimolar reactands (CO<sub>2</sub> and H<sub>2</sub>)  $\sqrt{c_0} - \sqrt{c}$  versus reaction time at 623 K in the inverse shift reaction

A nonlinear regression procedure using this equation (8) and all equimolar experiments produces parameter estimations for the formal reaction order  $n$ , the preexponential coefficient  $k_0$  and the activation energy  $E_a$ . The results of the nonlinear regression are shown in table 4. The preexponential factor  $k_0$  can not be seen as an absolute value, because it is dependent on the amount of catalyst, the form of the pellets, the catalyst's packing and the way the reaction time is calculated. But the relative values of  $k_0$  are characteristic in a physical-chemical sense. The reaction order  $n$  is a little bit smaller than the first assumed 0.5, but they are nearly identical for the shift reaction and the

Table 4: Kinetical parameter obtained by a nonlinear regression with the equimolar experimental data set for the watergas shift reaction and the inverse shift reaction

	$k_0$ [1/s]	$E_a$ [kJ/mol]	n
Shift Reaction	$2.3 \cdot 10^5$	54.4	0.38
Inverse Shift Reaction	$9 \cdot 10^5$	66.0	0.43

inverse shift reaction. The differences in the activation energies  $E_a$  are only about  $12 \text{ kJ/mol}$ , although the standard reaction energy  $\Delta H_r^\ominus$  for the water gas shift reaction is  $-44 \text{ kJ/mol}$ . The small difference in the experimental activation energies can be explained by the strong adsorption of water on the catalyst and the chemical reaction of the adsorbed species being rate determining.

### 3.3 Global modelling with all experimental results

Assuming a simple global reaction kinetics with a different fractional order for each substance, the 4 differential equations (9) together with its initial conditions are describing the reaction system completely.

$$\begin{aligned} \frac{d[\text{CO}]}{dt} &= \frac{d[\text{H}_2\text{O}]}{dt} = -\frac{d[\text{CO}_2]}{dt} = -\frac{d[\text{H}_2]}{dt} = \\ &= -k_f[\text{CO}]^{n_1}[\text{H}_2\text{O}]^{n_2} + k_b[\text{CO}_2]^{n_3}[\text{H}_2]^{n_4} \\ \text{with } k_f &= k_f^0 e^{-\frac{E_f}{RT}} \quad \text{and} \quad k_b = k_b^0 e^{-\frac{E_b}{RT}} \end{aligned} \quad (9)$$

The solution of these differential equations with arbitrary initial concentrations gives very complicated mathematical formulas or is not solvable in a closed analytical mathematical form. Therefore a numerical procedure for these equation was chosen. We used as a tool for all mathematical operations the MATLAB system. Assuming Arrhenius behaviour for the reaction rate constants  $k_f$  and  $k_b$  the differential equation solvers calculates the concentration in dependence on reaction time, if the initial concentrations at time  $t_0$  and all kinetical parameters are given.

From all the 266 experiments, we want to determine the kinetical parameters  $k_f^0$ ,  $E_f$ ,  $k_b^0$ ,  $E_b$ ,  $n_1$ ,  $n_2$ ,  $n_3$  and  $n_4$  (as shown in differential equation (9) in order to get an optimal agreement between the experiment values and the calculated ones. As an objective function the sum of the squares of the

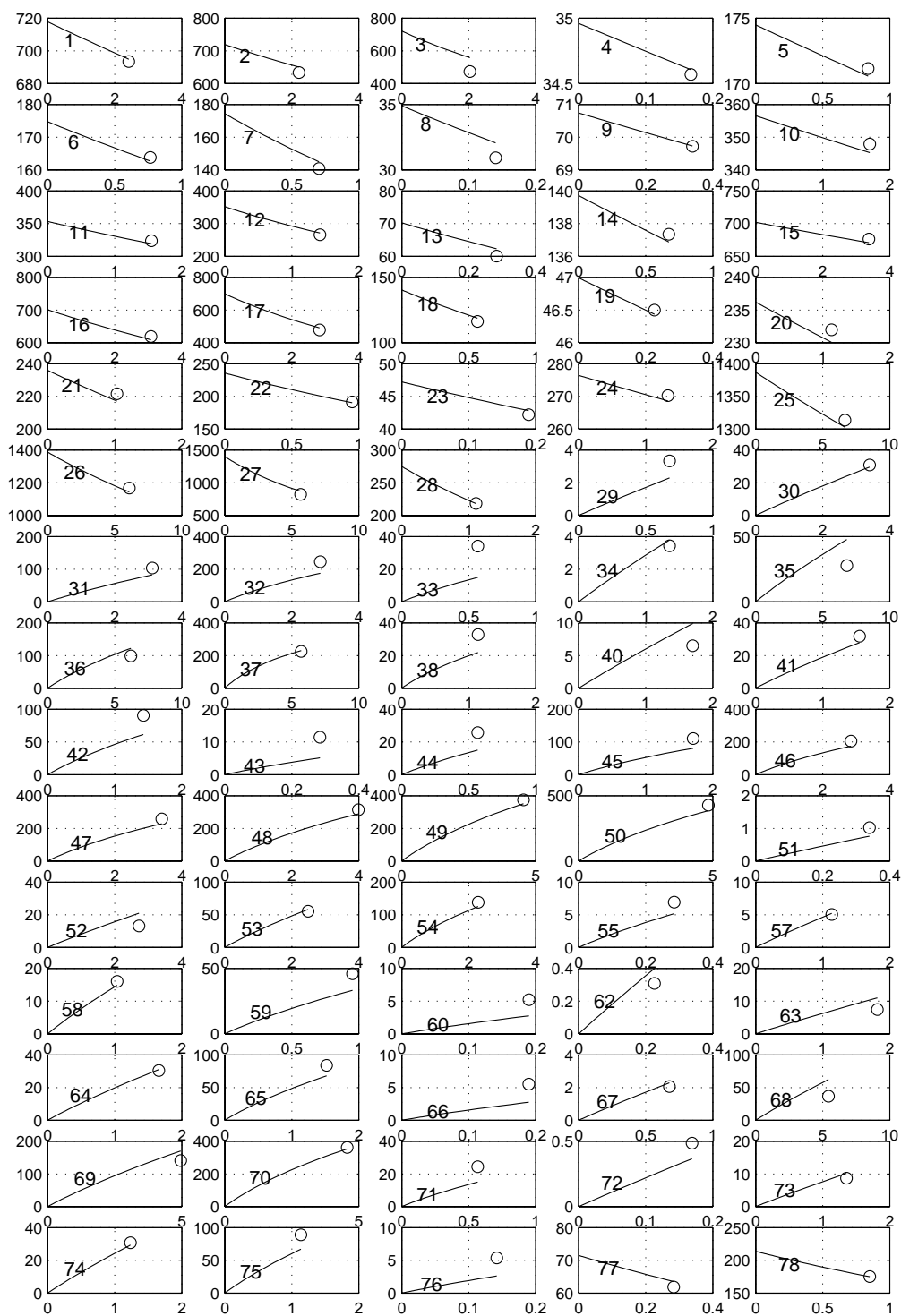


Figure 11: Modelling with global kinetics, experiments 1–78; the ordinate is the concentration of CO in mbar, the abscissa is the reaction time in seconds.

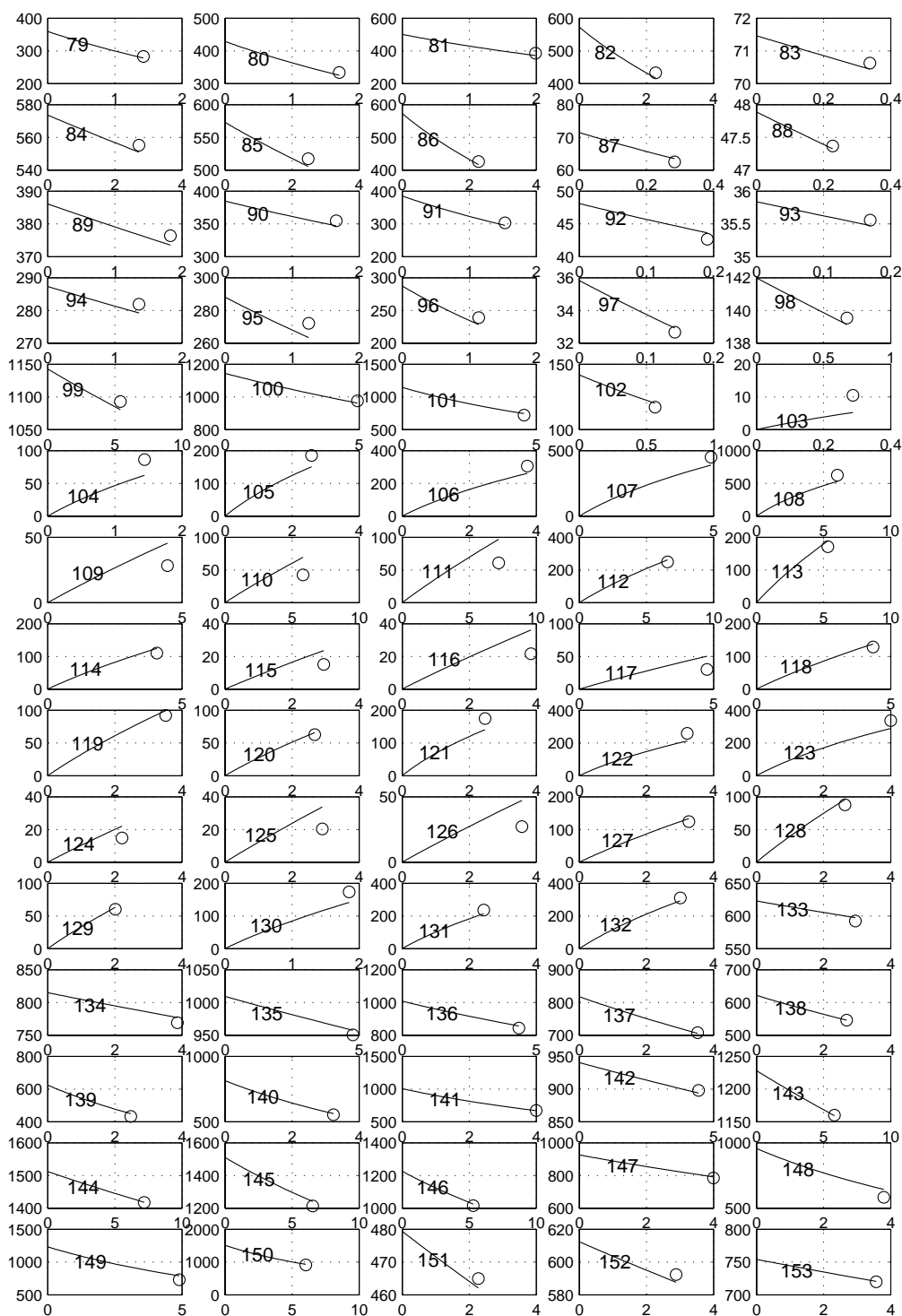


Figure 12: Modelling with global kinetics, experiments 79–153; the ordinate is the concentration of CO in mbar, the abscissa is the reaction time in seconds.



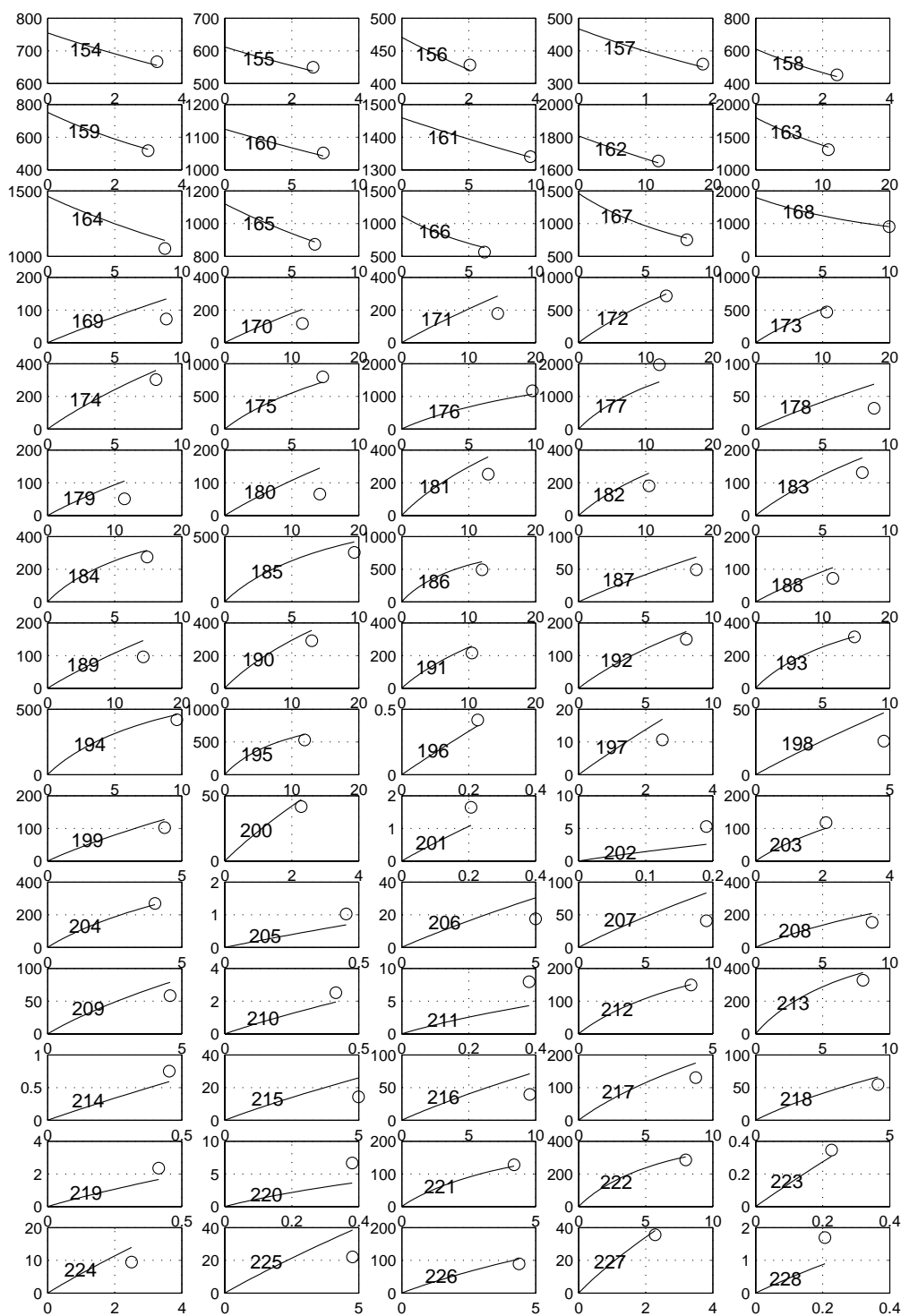


Figure 13: Modelling with global kinetics, experiments 154–228; the ordinate is the concentration of CO in mbar, the abscissa is the reaction time in seconds.

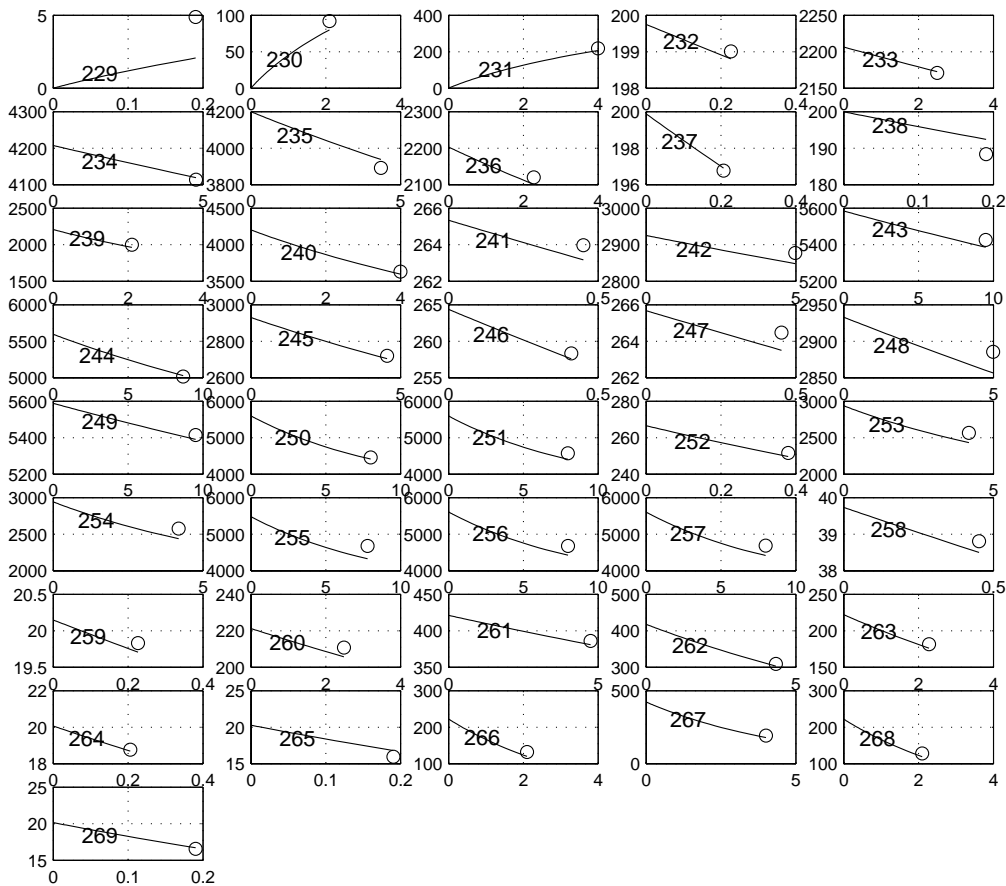


Figure 14: Modelling with global kinetics, experiments 229-269; the ordinate is the concentration of CO in mbar, the abscissa is the reaction time in seconds.

relative errors was used (equation 10) .

$$S = \sum_{i=1}^n \left( \frac{[\text{CO}]_{\text{calculated}} - [\text{CO}]_{\text{experimental}}}{[\text{CO}_2]_{\text{initial}} + [\text{CO}]_{\text{initial}}} \right)^2 \quad (10)$$

It is not necessary to use more than one substance in the objective function  $S$ , because the error of the other substances is the same. This originates from the way the experimental data in table 3 on page 12 are obtained to give a stoichiometric consistent data set. The squared error is summed over all experiments (sum counter  $i$ ) with all temperatures, all pressures, all different initial conditions and both types of reaction, the shift and the inverse shift reaction. For the optimization the simplex method was used in the form it is implemented in MATLAB. The results can be seen in figures 11, 12, 13 and

14 on pages 21, 22, 23 and 24.

The agreement is excellent. The average relative error is 2.07%. We omitted only three experiments at 250 °C, where we found no conversion. Considering the large range of initial conditions and the temperature range from a temperature with only minor conversions to a temperature, where the catalyst is just below the decomposition temperature, equation 9 on page 20 with the determined kinetical parameter can be used to calculate the kinetics of the water gas shift reaction and the inverse water gas shift reaction in a wide range of external parameters. The optimal kinetic parameters are compiled in table 5. Here again the activation energies for the shift reaction

Table 5: Optimal physical-chemical parameters for the global kinetics with fractional exponents as defined in equation (9) on page 20

	[1/mbar·s]		J/mol				
$k_f^0$	643000	$E_f$	62600	$n_1$	0.36	$n_2$	0.14
$k_b^0$	140000	$E_b$	61800	$n_3$	0.26	$n_4$	0.36

and the inverse shift reaction are nearly the same. The higher preexponential factor for the water gas shift reaction can be explained by the chemical equilibrium, which lies on the product side of CO<sub>2</sub> and H<sub>2</sub>. The exponents for the reactands and for the products sum up to 0.5 respectively 0.62, which is quite near the initial guess of 0.5, which was used for the interpretation of the equimolar experiments in section 3.2 on page 17. Of course optimization with many parameters may not be unambiguous and there are a lot of correlation effects between the parameters. This may even be worse for the following model calculations with more parameters. But the determined parameters should describe the experiments very well and they should be reasonable in respect to the physical chemical model used. And it should be reminded that an agreement between experimental and modelled data is a necessary condition and not a proof for the correctness of the model.

### 3.4 Modelling with a catalytic standard model using all experimental results

The standard model we used in this section assumes a bimolecular reaction of the adsorbed species in forward direction (water gas shift reaction) and a bimolecular reaction of the adsorbed species in backward reaction (inverse water gas shift reaction); [6]. The adsorbed species are in chemical equilibrium with its gaseous counterparts. There is only one sort of active site on

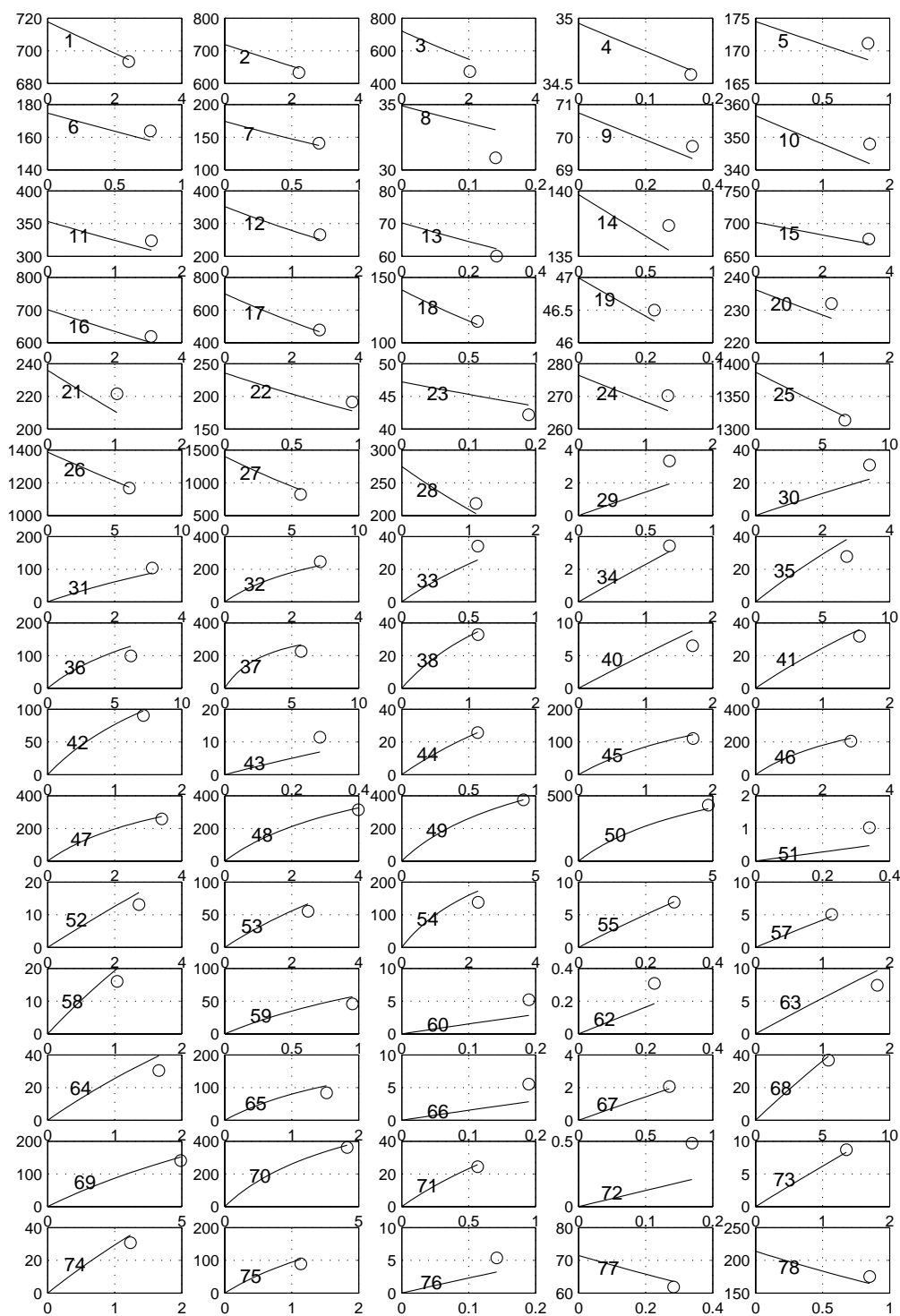


Figure 15: Modelling with Hinshelwood fractional kinetics, experiments 1–78; the ordinate is the concentration of CO in mbar, the abscissa is the reaction time in seconds.

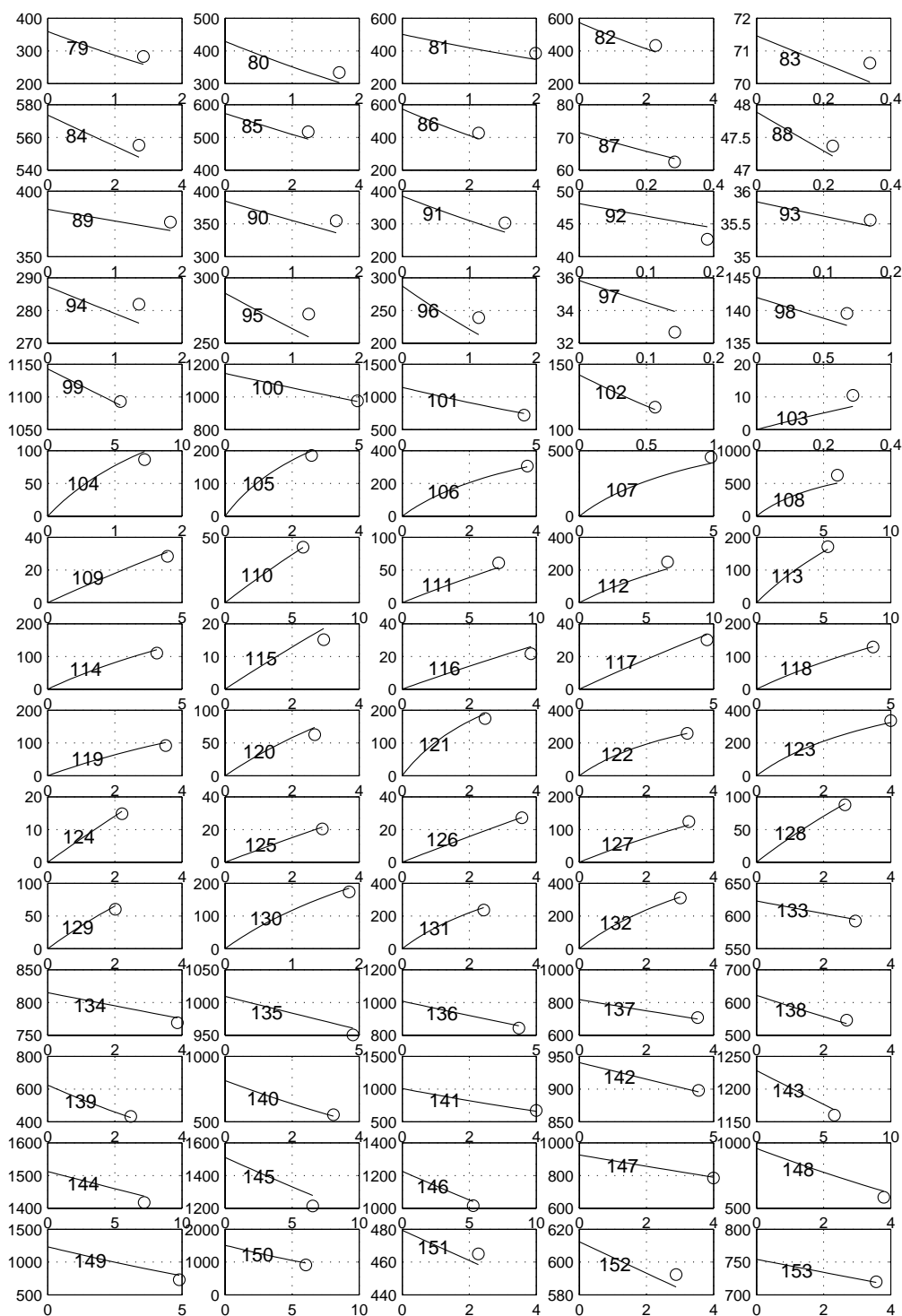


Figure 16: Modelling with Hinshelwood fractional kinetics, experiments 79–153; the ordinate is the concentration of CO in mbar, the abscissa is the reaction time in seconds.

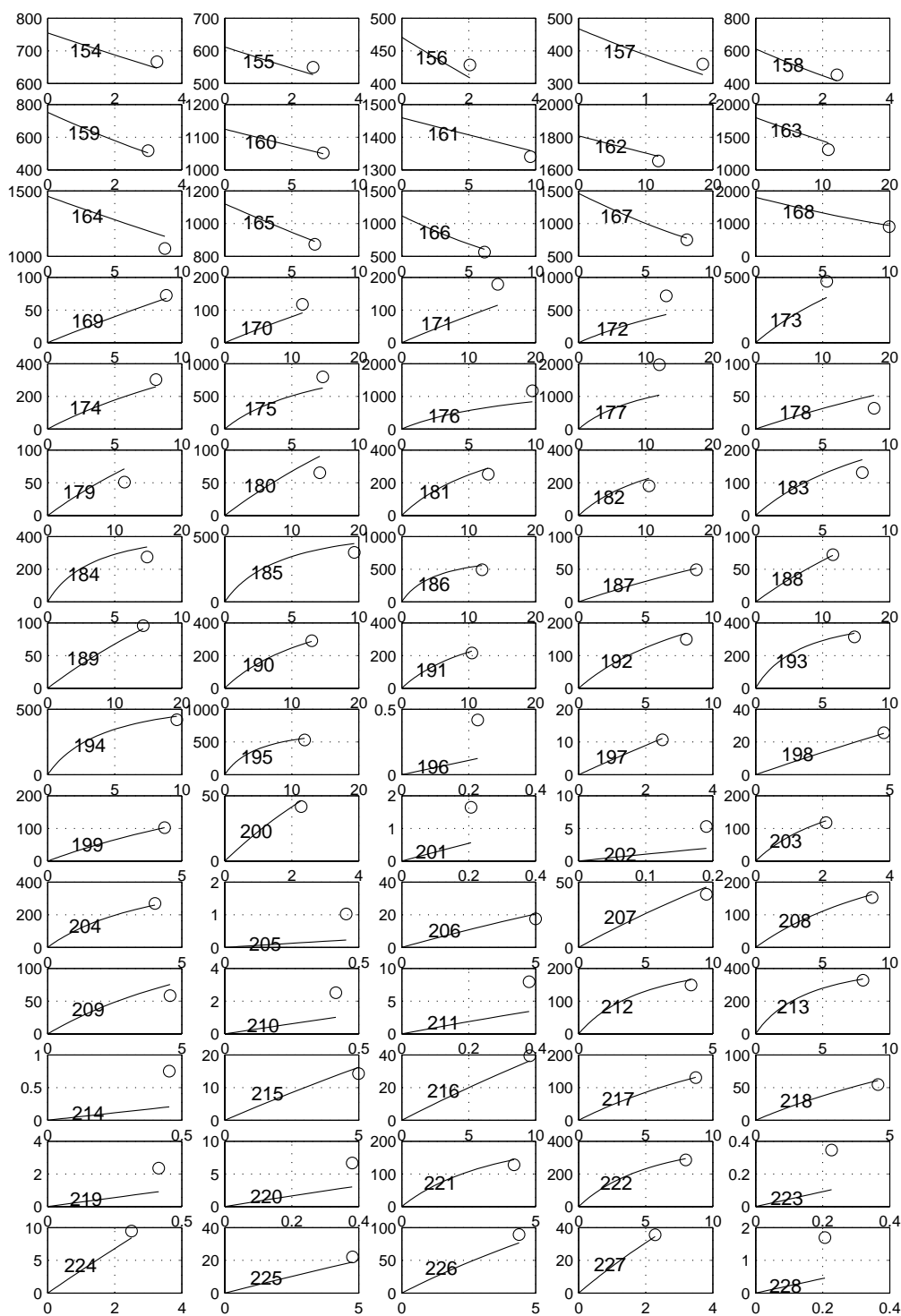


Figure 17: Modelling with Hinshelwood fractional kinetics, experiments 154–228; the ordinate is the concentration of CO in mbar, the abscissa is the reaction time in seconds.

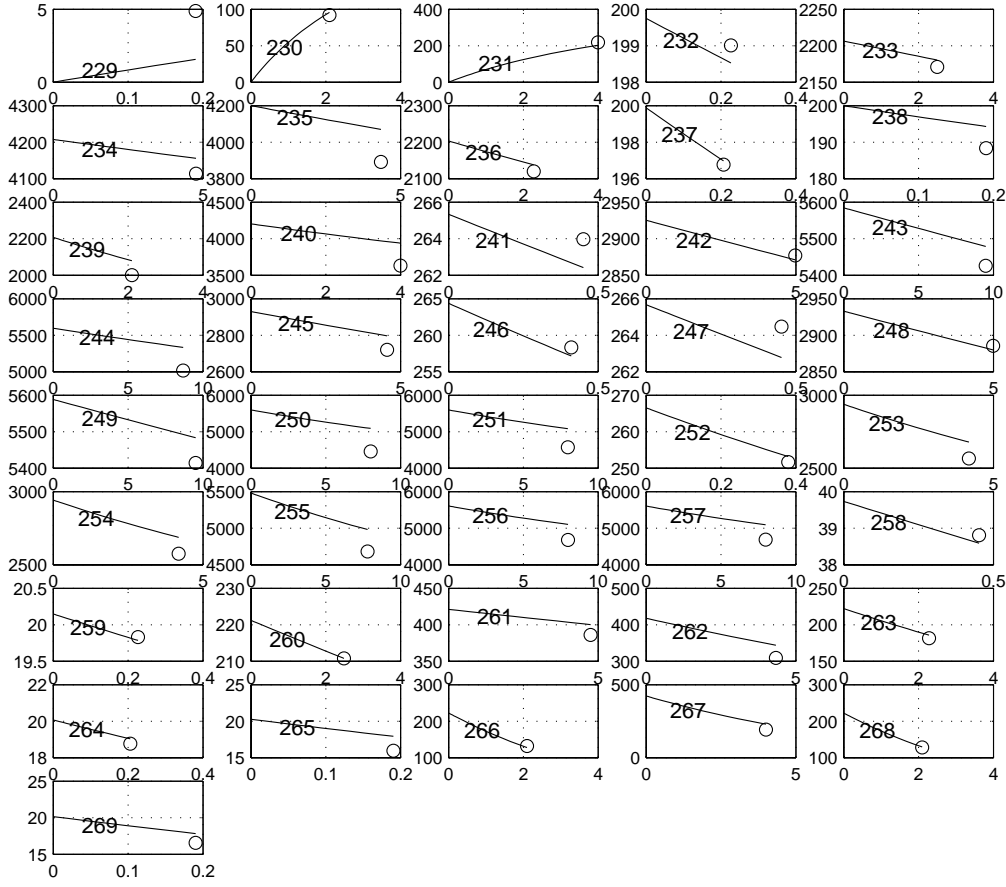


Figure 18: Modelling with Hinshelwood fractional kinetics, experiments 229-269; the ordinate is the concentration of CO in mbar, the abscissa is the reaction time in seconds.

the surface and all species are competing for the free active sites. The rate law shown in equation (11) can be derived from these postulations.

$$\begin{aligned}
 \frac{d[\text{CO}]}{dt} &= \frac{d[\text{H}_2\text{O}]}{dt} = -\frac{d[\text{CO}_2]}{dt} = -\frac{d[\text{H}_2]}{dt} = \\
 &= \frac{-k_f[\text{CO}][\text{H}_2\text{O}] + k_b[\text{CO}_2][\text{H}_2]}{(1 + K_1[\text{CO}] + K_2[\text{H}_2\text{O}] + K_3[\text{CO}_2] + K_4[\text{H}_2])^2} \\
 &\quad \text{with } k_f = k_f^0 e^{-\frac{E_f}{RT}} \quad \text{and} \quad k_b = k_b^0 e^{-\frac{E_b}{RT}} \\
 &\quad \quad \quad \text{with } K_i = K_i^0 e^{-\frac{E_i}{RT}} \quad (11)
 \end{aligned}$$

The parameters  $K_1$ ,  $K_2$ ,  $K_3$  and  $K_4$  are the formal equilibrium constants for the adsorption/desorption equilibrium of the respective species.

$$K = K_0 \exp\left(\frac{+E_a}{RT}\right) = \frac{\theta_c}{c \cdot \theta} \quad (12)$$

In the equation (12)  $c$  is the gas concentration of a substance,  $\theta$  is the fraction of free active surface sites and  $\theta_c$  is the fraction of active surface sites which is covered by this substance. For the temperature dependence of these constants an Arrhenius law is assumed but with a positive sign in the exponential. The equation (11) has to be solved numerically. The same differential equation solver and the same optimization procedure as in section (3.3) with the same objective function (equation 10 on page 24 ) was used. The results can be seen in figures 15, 16, 17 and 18 on pages 26, 27, 28 and 29. Again the agreement between the experimental and the calculated concentrations is excellent. The average relative error is now 3.02%. This is greater than the 2% of the global model, but the differences can hardly be seen in the figures. The optimal kinetic parameters for the optimization with equation (11) are compiled in table 6 on page 30. In this table the activation energies

Table 6: Optimal physical-chemical parameters catalytical standard kinetics with Hinshelwood assumptions as defined in equation ( 11) on page 29

	$k_i^0$ or $K_i^0$	$E_a$ J/mol
Shift reaction $k_f$	71.8 $1/\text{mbar} \cdot \text{t}$	41170
InverseShift reaction $k_b$	7108 $1/\text{mbar} \cdot \text{t}$	78960
CO adsorption $K_1$	$7.150 \cdot 10^{-3}$ $1/\text{mbar}$	46
H <sub>2</sub> O adsorption $K_2$	$0.277 \cdot 10^{-3}$ $1/\text{mbar}$	17490
H <sub>2</sub> adsorption $K_3$	$1.774 \cdot 10^{-3}$ $1/\text{mbar}$	0
CO <sub>2</sub> adsorption $K_4$	$0.591 \cdot 10^{-3}$ $1/\text{mbar}$	3610

of the forward and backward reaction differ nearly 40 kJ which corresponds approximatively the reaction enthalpie. The adsorption energy of water is with 17.5 kJ the distinct highest value. The strong adsorption of water is in accordance with our laboratory experience.



### 3.5 Modelling the Hinshelwood kinetics in the form of elementary reactions

In table 7 on page 31 the most simple reaction mechanism for the Hinshelwood mechanism in the form of elementary reactions is written down: There

Table 7: Reaction mechanism for a simple Hinshelwood kinetics including adsorption desorption kinetics

$k_1$	$\text{CO}$	+	$\text{O}$	$\longrightarrow$	$\text{CO}^{\text{ads}}$		
$k_2$	$\text{CO}^{\text{ads}}$			$\longrightarrow$	$\text{CO}$	+	$\text{O}$
$k_3$	$\text{CO}_2$	+	$\text{O}$	$\longrightarrow$	$\text{CO}_2^{\text{ads}}$		
$k_4$	$\text{CO}_2^{\text{ads}}$			$\longrightarrow$	$\text{CO}_2$	+	$\text{O}$
$k_5$	$\text{H}_2\text{O}$	+	$\text{O}$	$\longrightarrow$	$\text{H}_2\text{O}^{\text{ads}}$		
$k_6$	$\text{H}_2\text{O}^{\text{ads}}$			$\longrightarrow$	$\text{H}_2\text{O}$	+	$\text{O}$
$k_7$	$\text{H}_2$	+	$\text{O}$	$\longrightarrow$	$\text{H}_2^{\text{ads}}$		
$k_8$	$\text{H}_2^{\text{ads}}$			$\longrightarrow$	$\text{H}_2$	+	$\text{O}$
$k_9$	$\text{CO}^{\text{ads}}$	+	$\text{H}_2\text{O}^{\text{ads}}$	$\longrightarrow$	$\text{CO}_2^{\text{ads}}$	+	$\text{H}_2^{\text{ads}}$
$k_{10}$	$\text{CO}_2^{\text{ads}}$	+	$\text{H}_2^{\text{ads}}$	$\longrightarrow$	$\text{CO}^{\text{ads}}$	+	$\text{H}_2\text{O}^{\text{ads}}$

are 4 adsorption reactions, 4 desorption reactions and two chemical reactions at the surface, but there are no diffusions or surface diffusions as transport considered. The transport is assumed to be infinitely fast. The chemical reaction mechanism can easily be converted to the system of differential equation of order 9; 4 for the adsorbed species, 4 for the gases and 1 for the surface sites. This is done with a MATLAB program (see page 39 in the appendix section 4.2) to obtain another MATLAB program which contains the system of differential equation in a usable form.

A modification has to be applied. Only the gaseous species remain differential equations, the other ones have to be converted to algebraic equations, which are set to zero. This can be explained considering the partial differential equation for a gas  $c$  flowing with a flow rate  $v$  through a fixed bed, being adsorbed and reacting as adsorbed species  $\bar{c}$  with first order at the surface to gaseous products. Only the dependence on time  $t$  and length  $l$  are considered. The equations for  $c$ ,  $\bar{c}$  and surface sites  $O$  are written down in equation (13); the reaction constants are  $k_a$  for the adsorption,  $k_d$  for the

desorption and  $k_r$  for the reaction.

$$\begin{aligned}
\frac{\partial c(l, t)}{\partial t} &= -k_a c(l, t)O(l, t) - v \frac{\partial c(l, t)}{\partial l} + k_d \bar{c}(l, t) \\
\frac{\partial O(l, t)}{\partial t} &= -k_a c(l, t)O(l, t) + k_d \bar{c}(l, t) \\
\frac{\partial \bar{c}(l, t)}{\partial t} &= k_a c(l, t)O(l, t) - k_d \bar{c}(l, t) - k_r \bar{c}(l, t)
\end{aligned} \tag{13}$$

If the flow reactor is stationary, no time dependence remains and the equation (13) can be rewritten as equation (14).

$$\begin{aligned}
0 &= -k_a c(l, t)O(l, t) - v \frac{\partial c(l, t)}{\partial l} + k_d \bar{c}(l, t) \\
0 &= -k_a c(l, t)O(l, t) + k_d \bar{c}(l, t) \\
0 &= k_a c(l, t)O(l, t) - k_d \bar{c}(l, t) - k_r \bar{c}(l, t)
\end{aligned} \tag{14}$$

Equation (14) can now be rewritten as an algebraic differential equation system. It is usual to substitute the variable  $l$  by the variable  $t$  using the relation  $l = vt$ ;  $t$  now means the residence time of a particle at a certain point  $l$  of the reactor. The result is equation (15).

$$\begin{aligned}
\frac{dc(t)}{dt} &= -k_a c(t)O(t) + k_d \bar{c}(t) \\
0 &= -k_a c(t)O(t) + k_d \bar{c}(t) \\
0 &= k_a c(t)O(t) - k_d \bar{c}(t) - k_r \bar{c}(t)
\end{aligned} \tag{15}$$

For such systems a numerical solver for algebraic differential equation systems is needed. For the resulting algebraic differential equation system of our mechanism the MATLAB solver didn't work satisfactorily. An alternative is the using of a stiff solver for differential equations and writing the algebraic equations as differential equations, but applying to them an additional factor, making these equations very fast. This is the same method used in the quasi stationary state assumption to transform a differential equation in an algebraic one. By this method we solved the reaction kinetics. The same optimization procedure as in section (3.3) with the same objective function (equation 10 on page 24) was used. The 4 adsorption reactions, the 4 desorption reactions and the 2 chemical reactions have each an preexponential factor and an activation energy. In addition the 'concentration' of the active surface sites is unknown. Therefore 21 parameters had to be determined. With the MATLAB main program `hauptprogramm.m` (see page 44 in the appendix section 4.2.4) the optimization is started. The programs called by

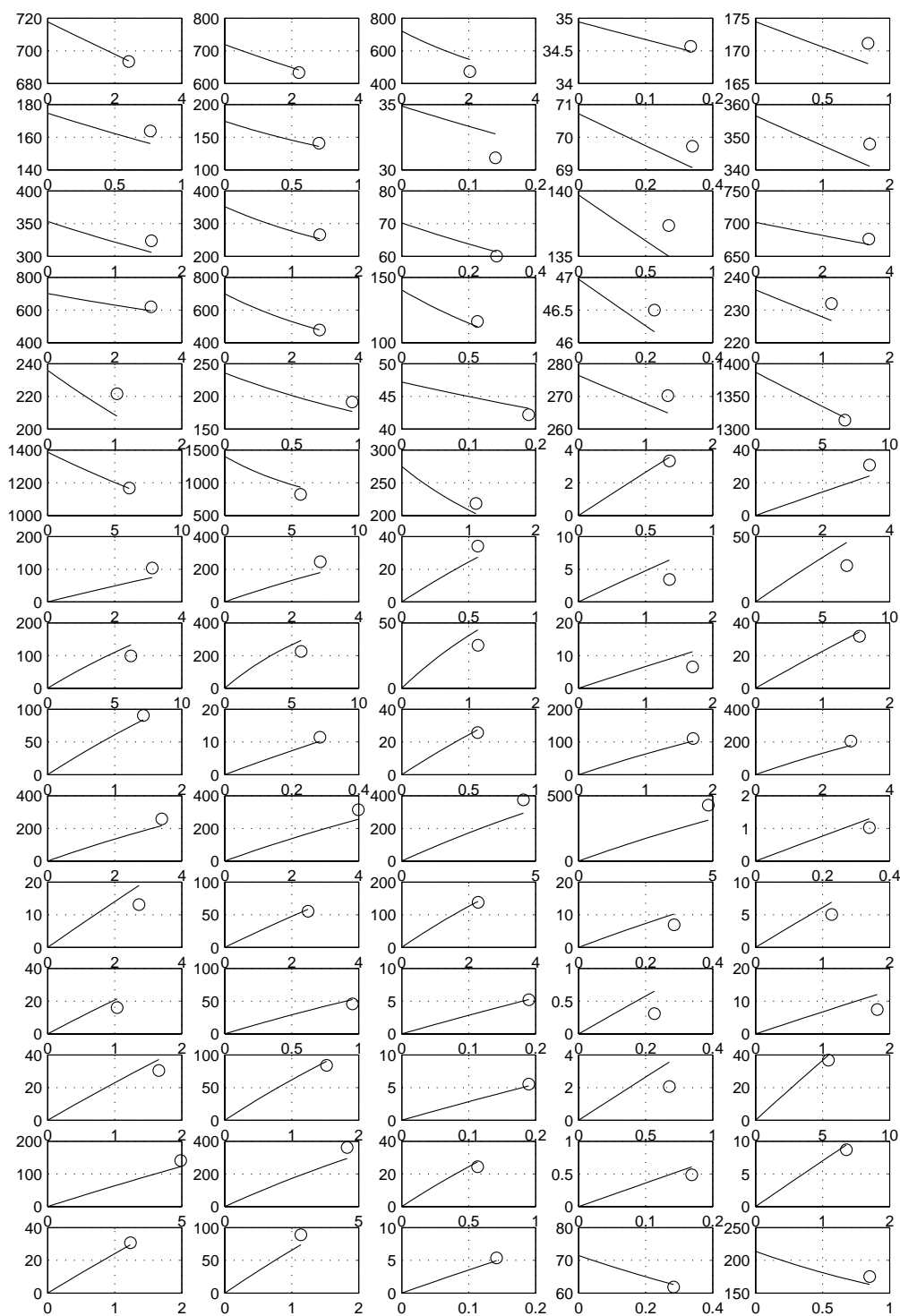


Figure 19: Modelling with elementary reactions according to the Hinshelwood mechanism, experiments 1-78; the ordinate is the concentration of CO in mbar, the abscissa is the reaction time in seconds.

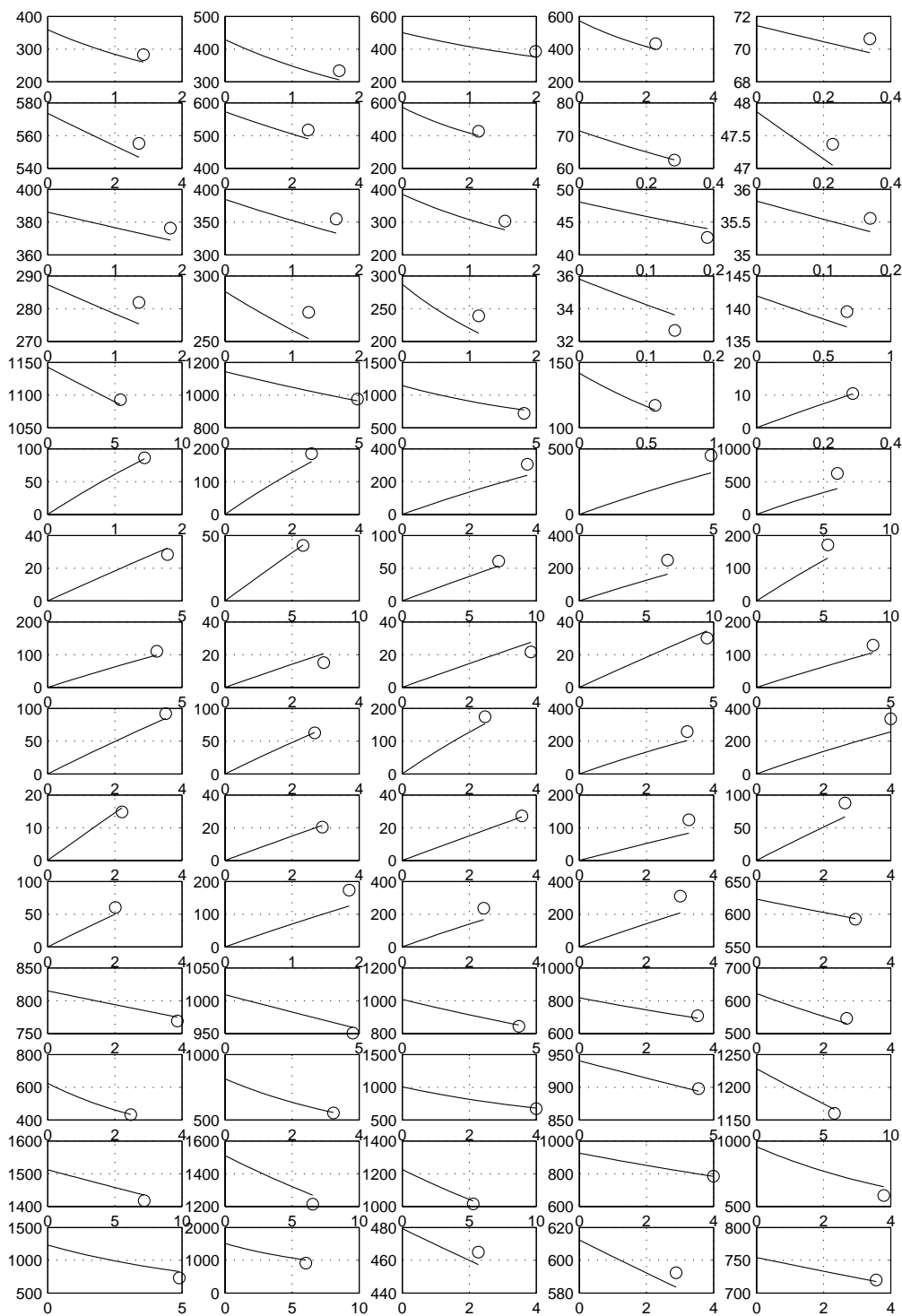


Figure 20: Modelling with elementary reactions according to the Hinshelwood mechanism, experiments 79–153; the ordinate is the concentration of CO in mbar, the abscissa is the reaction time in seconds.

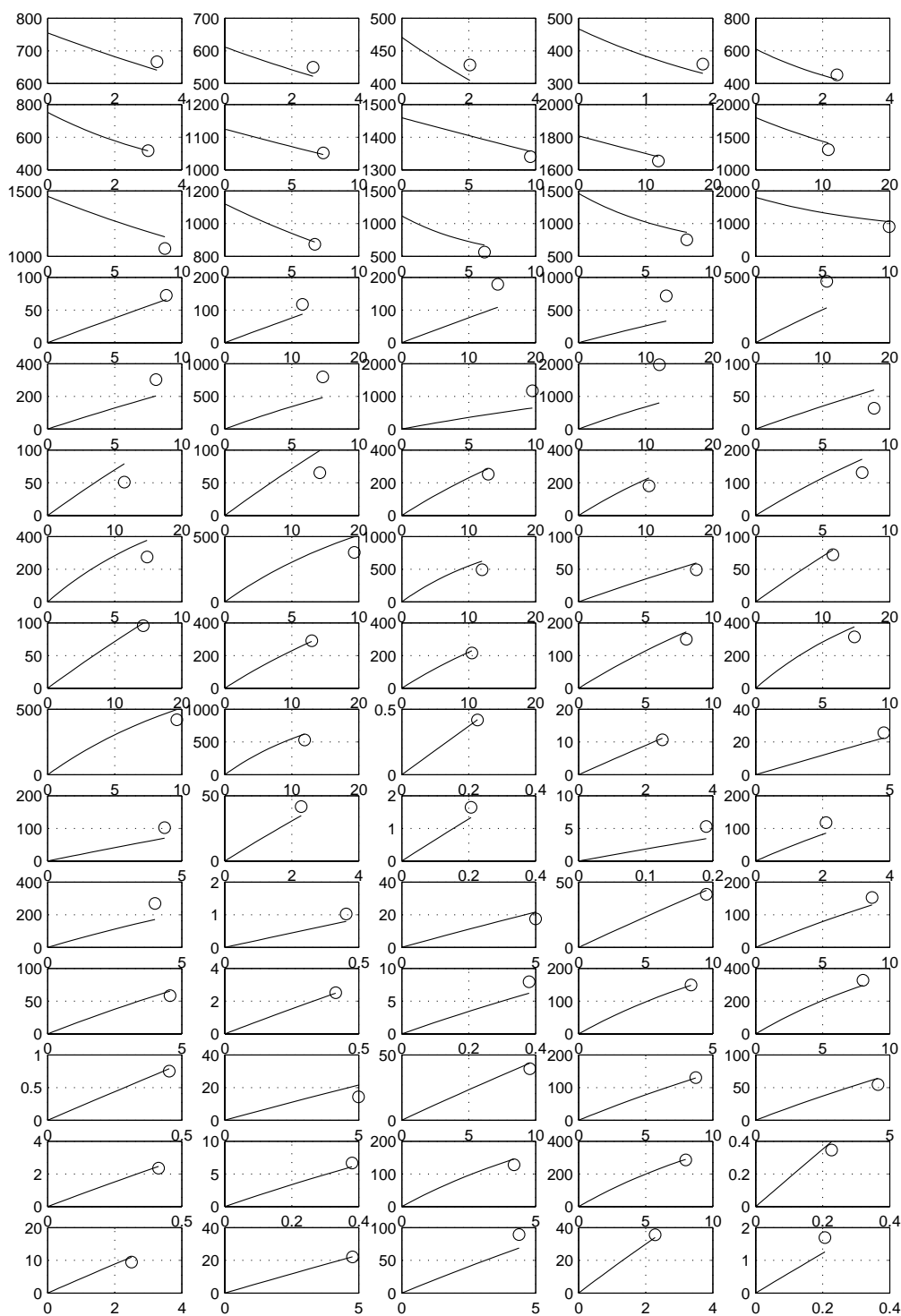


Figure 21: Modelling with elementary reactions according to the Hinshelwood mechanism, experiments 154–228; the ordinate is the concentration of CO in mbar, the abscissa is the reaction time in seconds.

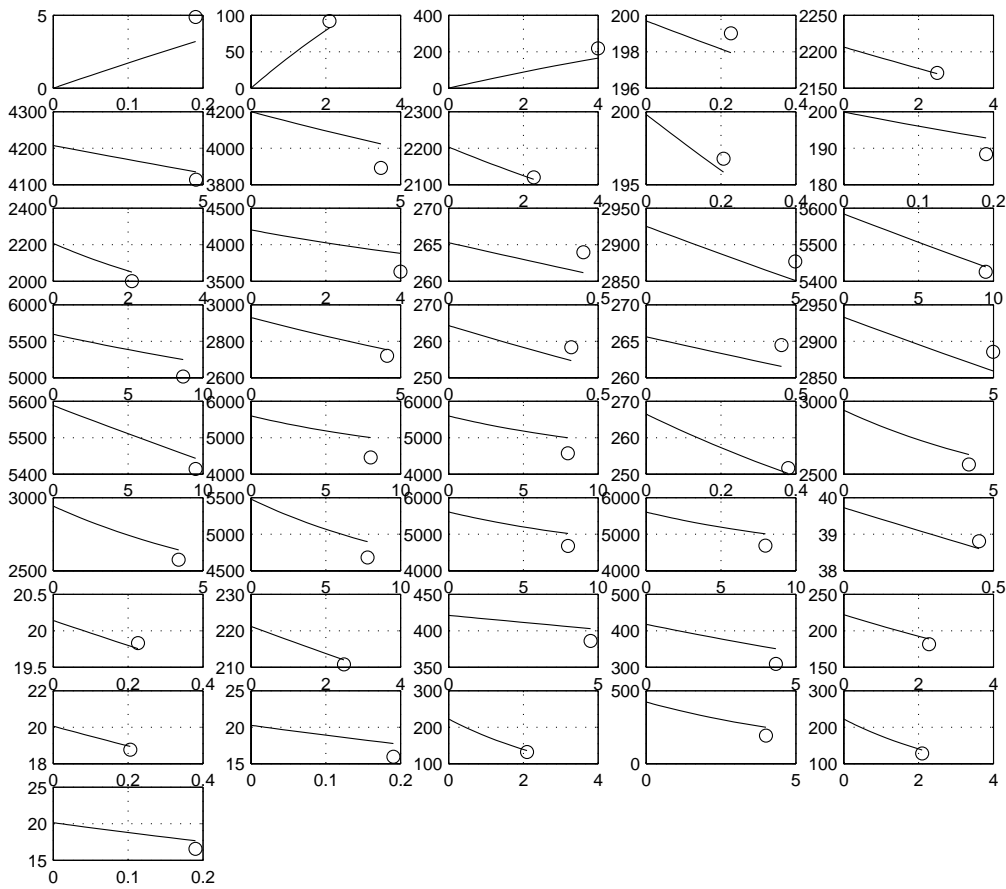


Figure 22: Modelling with elementary reactions according to the Hinshelwood mechanism, experiments 229-269; the ordinate is the concentration of CO in mbar, the abscissa is the reaction time in seconds.

the main program are also listed in the appendix. The results can be seen in figures 19, 20, 21 and 22 on pages 33, 34, 35 and 36. Again the agreement between the experimental and the calculated concentrations is very good. The average relative error is now 3.23%. This is nearly the same as calculated in the catalytic standard model.

The optimal kinetic parameters for the optimization of the elementary reaction mechanism given in table 7 on page 31 are compiled in table 8 on page 37.

In table 8 it can be seen, that the activation energies of the two surface reactions (forwards and backwards) are again nearly the same. Within the adsorption/desorption reaction steps only the desorption of water has a relevant activation energy. There is an additional free parameter, which has

Table 8: Optimal kinetical parameters  $k_i^0$  (in  $1/s$  if the reaction is first order or  $1/\text{mbar} \cdot s$  if the reaction is second order) and  $E_i$  (in  $\text{J/mol}$ ) of the elementary reaction mechanism given in table 7 on page 31. An additional parameter, the concentration of the active sites, has been calculated as 161 mbar .

	$k_i^0$	$E_i$	
$k_1$	4.17	0	$\text{CO} + \text{O} \longrightarrow \text{CO}^{\text{ads}}$
$k_2$	719	255	$\text{CO}^{\text{ads}} \longrightarrow \text{CO} + \text{O}$
$k_3$	6.21	0	$\text{CO}_2 + \text{O} \longrightarrow \text{CO}_2^{\text{ads}}$
$k_4$	1264	655	$\text{CO}_2^{\text{ads}} \longrightarrow \text{CO}_2 + \text{O}$
$k_5$	0.171	0	$\text{H}_2\text{O} + \text{O} \longrightarrow \text{H}_2\text{O}^{\text{ads}}$
$k_6$	1071	21201	$\text{H}_2\text{O}^{\text{ads}} \longrightarrow \text{H}_2\text{O} + \text{O}$
$k_7$	6.49	0	$\text{H}_2 + \text{O} \longrightarrow \text{H}_2^{\text{ads}}$
$k_8$	1201	260	$\text{H}_2^{\text{ads}} \longrightarrow \text{H}_2 + \text{O}$
$k_9$	1220	56928	$\text{CO}^{\text{ads}} + \text{H}_2\text{O}^{\text{ads}} \longrightarrow \text{CO}_2^{\text{ads}} + \text{H}_2^{\text{ads}}$
$k_{10}$	2517	63145	$\text{CO}_2^{\text{ads}} + \text{H}_2^{\text{ads}} \longrightarrow \text{CO}^{\text{ads}} + \text{H}_2\text{O}^{\text{ads}}$

been determined by the optimization procedure: a formal concentration of the active sites of 161 mbar has been obtained.

### 3.6 Catalyst poisoning

We performed a poisoning experiment with HCl in a separate quartz apparatus. For this we used 1% HCl in He. At 350 °C 30 ml<sup>n</sup>/min of the gas mixture was lead over catalyst. After 12 hour 1.1 g HCl had flown through 1 g of the catalyst. Then the catalytic activity was reduced by 52%. After a first resulfidation the activation was restored to 92.2% of the initial activity. After a second resulfidation the initial activity was completely restored.

## 4 Appendices

### 4.1 Catalyst activation and resulfidation

A modified instruction to sulfidate the catalyst CoMo\_C49 of Süd-Chemie company; [7].

1. The catalyst pellets are heated up to 350 °C with a temperature gradient of 10 °C/min in an Ar flow of 50 mln/min at atmospheric pressure until most of the adsorbed gases are desorbed. The temperature 350 °C is held until the concentration of water in the outlet is less than 1ppm.
2. afterwards the catalyst is cooled down to room temperature still using Ar as protection gas.
3. a H<sub>2</sub>-flow of 50 mln/min containing 0.3% H<sub>2</sub>S is flowing over the catalyst and the temperature is increased with 0.5 °C/min until the end temperature of 210 °C is reached.
4. the temperature of 210 °C is held constant and the flow of H<sub>2</sub>-flow containing 0.3% H<sub>2</sub>S is continued until the concentration of H<sub>2</sub>S in the outflow is constant at 0.3%.
5. then the sulfidation is continued with a temperature increase of 0.23 °C/min until the temperature of 357 °C is reached. The sulfidation at this maximum temperature is continued until the concentration of H<sub>2</sub>S in the outflow is constant at 0.3% or a maximum of 2 hours is exceeded.
6. then the catalyst is cooled down in an Ar gas flow of 50 mln/min and stored.

The just prepared catalyst is tested with constant experimental parameters with the inverse watergas shift reaction und the resulting conversion is defined as 100% activity. After the catalyst has been used for some weeks its activity is examined. If the activity is reduced then the catalyst will be resulfidated after the following modified instructions.

- after step 1 the temperature is slowly increased to 357 °C
- at 357 °C an equimolar mixture of H<sub>2</sub>-Ar containing 0.3% H<sub>2</sub>S with a total feed of 50 mln/min is flowing over the catalyst
- the sulfidation at 357 °C is continued until the concentration of H<sub>2</sub>S in the outflow is constant at 0.3%
- then the catalyst is cooled down in an Ar gas flow of 50 mln/min and stored.

In a catalytic reaction experiment some sulfur compounds can be found in the outlet gas: H<sub>2</sub>S, SO, SO<sub>2</sub> and COS. The highest concentrations are measured for H<sub>2</sub>S for high residence times and if CO is used in surplus,



but are still smaller than 10 ppm . Using equimolar reactands the loss of S is only half of the sulfur-atoms if the experiment is continued for some months. The recommendation of the manufacturer is to use 30–50 ppm H<sub>2</sub>S in the reaction gases. We did not follow it. But nevertheless we resulfidated the catalyst every 4–6 weeks although we did not measure any decrease of catalyst activity.

## 4.2 Computer programs

### 4.2.1 mehdiff.m

A MATLAB program mehdiff.m to convert a chemical mechanism to a system of ordinary differential equation as a MATLAB program usable with the MATLAB solvers for differential equations.

```
%MATLAB script mehdiff.m
ss=textread('shift02.txt','%s','delimiter','\n','whitespace','') ;
s=strrep(ss,' ','');
s=strrep(s,'=','');
n=length(s);
left=1;right=1;clear left right;
lnums=zeros(n,1);rnums=zeros(n,1);
for i=1:n
    [left{i}, right{i}]=strtok(s{i}, '>');
end;
left=transpose(left) ;
right=transpose(right) ;
right=strrep(right, '>', '');

for i=1:n

    flag=1;j=0;
    sh=left{i};
    while flag==1;
        flag=0;j=j+1;
        [ a b]=strtok(sh, '+') ;
        lsubs(i,j)=cellstr(a);
        if prod(size(b))>0
            sh=strrep(b, '+', '');flag=1;
        end
    end;
    lnums(i,1)=j;
end;
```

```

flag=1;j=0;
sh=right{i};
while flag==1;
    flag=0;j=j+1;
    [ a b]=strtok(sh, '+') ;
    rsubs(i,j)=cellstr(a);
    if prod(size(b))>0
        sh=strrep(b, '+', '');flag=1;
    end
end;
rnums(i,1)=j;
end;

sh=sort(reshape([lsubs rsubs],prod(size([lsubs rsubs])),1));

j=1;
for i=1:length(sh)
    if iscellstr(sh(i))==1 ;
        shh(j)=sh(i);j=j+1;
    end;
end
clear sh;

j=1;sh(1)=shh(1);
for i=2:length(shh)
    if strcmp(sh(j),shh(i))==0 ;
        j=j+1;
        sh(j)=shh(i);
    end;
end
sh=transpose(sh);
ndiff=length(sh);

for i=1:ndiff
    for j=1:n
        for k=1:lnums(j)
            if strcmp(lsubs(j,k),sh(i))==1
                lsubn(j,k)=i;
            end
        end
    end
end

```

```

        end
    end
    for j=1:n
        for k=1:rnums(j)
            if strcmp(rsubs(j,k),sh(i))==1
                rsubn(j,k)=i;
            end
        end
    end
end
end
% Ausgabe des ODE-Systems
fid = fopen('dgl.m', 'w');
fprintf(fid, 'function dydt = dgl(t,y,k) \n\n ');
fprintf(fid, '%%Reaktionsmechanismus \n');
for i=1:n
    a=char(ss(i));
    fprintf(fid, '%%(%3i)    %1s\n', i, a);
end
fprintf(fid, '\n\n%%Zuordnung der Variablen zu den Namen \n');
for i=1:ndiff
    a=char(sh(i));
    if a(1)~='Z';
        iz=i;
    end
    fprintf(fid, '%%y(%3i) = %1s \n', i, a);
end
iz=iz+1;
%fprintf(fid, '\n\n iz = %3i\n\n', iz);
fprintf(fid, '\n\nneins=1.0;\n\n');
fprintf(fid, '\n\n%%Reaktionsgeschwindigkeiten\n');
for i=1:n
    fprintf(fid, 'r(%3i) = k(%3i)', i, i);
    jende=lnums(i);
    for j=1:jende
        fprintf(fid, '*y(%3i)', lsubn(i, j));
    end
    fprintf(fid, ';\n');
end
fprintf(fid, '\n\n%%Differentialgleichungen\n');
for i=1:ndiff
    fprintf(fid, 'dydt(%3i) = ', i);

```

```

for j=1:n
    for k=1:lnums(j)
        if i==lsubn(j,k)
            fprintf(fid, '-r(%3i)', j);
        end
    end
    for k=1:rnums(j)
        if i==rsubn(j,k)
            fprintf(fid, '+r(%3i)', j);
        end
    end
end
fprintf(fid, '; \n');
if i>=iz
    fprintf(fid, 'dydt(%3i) = eins * dydt(%3i); \n', i, i);
end
end
fprintf(fid, 'dydt=transpose(dydt); \n');
fclose(fid);

```

#### 4.2.2 shift02.txt

The next is the data file `shift02.txt`, where the mechanism is formulated. This file is used as the input file for the MATLAB function `mechdiff.m`

```

C0    +    Z           ==>  Z_C0
Z_C0           ==>  C0      +    Z
C02    +    Z           ==>  Z_C02
Z_C02           ==>  C02    +    Z
H20    +    Z           ==>  Z_H20
Z_H20           ==>  H20    +    Z
H2     +    Z           ==>  Z_H2
Z_H2           ==>  H2     +    Z
Z_C0  +    Z_H20        ==>  Z_C02  +    Z_H2
Z_C02 +    Z_H2         ==>  Z_C0   +    Z_H20

```

#### 4.2.3 dgl.m

The output file is called `dgl.m` and is directly usable as a MATLAB function.

```

function dydt = dgl(t,y,k)

%Reaktionsmechanismus
%( 1)  CO +  Z  ==>  Z_CO
%( 2)  Z_CO ==>  CO+ Z
%( 3)  CO2+  Z  ==>  Z_CO2
%( 4)  Z_CO2 ==>  CO2+ Z
%( 5)  H2O + Z ==> Z_H2O
%( 6)  Z_H2O      ==>  H2O + Z
%( 7)  H2 + Z ==> Z_H2
%( 8)  Z_H2      ==>  H2 + Z
%( 9)  Z_CO + Z_H2O ==> Z_CO2 + Z_H2
%( 10) Z_CO2+Z_H2==>Z_CO+Z_H2

%Zuordnung der Variablen zu den Namen
%y( 1) = CO
%y( 2) = CO2
%y( 3) = H2
%y( 4) = H2O
%y( 5) = Z
%y( 6) = Z_CO
%y( 7) = Z_CO2
%y( 8) = Z_H2
%y( 9) = Z_H2O

eins=1000.0;

%Reaktionsgeschwindigkeiten
r( 1) = k( 1)*y( 1)*y( 5);
r( 2) = k( 2)*y( 6);
r( 3) = k( 3)*y( 2)*y( 5);
r( 4) = k( 4)*y( 7);
r( 5) = k( 5)*y( 4)*y( 5);
r( 6) = k( 6)*y( 9);
r( 7) = k( 7)*y( 3)*y( 5);
r( 8) = k( 8)*y( 8);
r( 9) = k( 9)*y( 6)*y( 9);

```

```
r( 10) = k( 10)*y( 7)*y( 8);
```

```
%Differentialgleichungen
```

```
dydt( 1) = -r( 1)+r( 2);
```

```
dydt( 2) = -r( 3)+r( 4);
```

```
dydt( 3) = -r( 7)+r( 8);
```

```
dydt( 4) = -r( 5)+r( 6);
```

```
dydt( 5) = -r( 1)+r( 2)-r( 3)+r( 4)-r( 5)+r( 6)-r( 7)+r( 8);
```

```
dydt( 5) = eins * dydt( 5);
```

```
dydt( 6) = +r( 1)-r( 2)-r( 9)+r( 10);
```

```
dydt( 6) = eins * dydt( 6);
```

```
dydt( 7) = +r( 3)-r( 4)+r( 9)-r( 10);
```

```
dydt( 7) = eins * dydt( 7);
```

```
dydt( 8) = +r( 7)-r( 8)+r( 9)-r( 10);
```

```
dydt( 8) = eins * dydt( 8);
```

```
dydt( 9) = +r( 5)-r( 6)-r( 9)+r( 10);
```

```
dydt( 9) = eins * dydt( 9);
```

```
dydt=transpose(dydt);
```

#### 4.2.4 hauptprogramm.m

The MATLAB script `hauptprogramm.m` starts the optimization routine reading the experimental data and user supplied guesses of the parameter and calling the minimum search routine for the objective function.

```
%hauptprogramm.m
```

```
global DATEN ZWISCHEN;
```

```
ZWISCHEN=[];
```

```
[kennnummer kelvin druck zeit fco fh2o fh2 fco2 co co2 h2 h2o ] = ...
```

```
    textread('versuche04.txt','%f %f %f %f %f %f %f %f %f %f %f %f',...
```

```
    'headerlines',1);
```

```
zusammen=[kennnummer kelvin druck zeit fco fh2o fh2 fco2 co co2 h2 h2o ];
```

```
%zum Beispiel Temperatúrauswahl 623 und hin-Reaktion
```

```
    % reduziert=zusammen(zusammen(:,2)== 623,:);
```

```
    %reduziert=reduziert(reduziert(:,5)>0,:);
```

```
DATEN = zusammen;
```

```
options = optimset('Display','iter');
```

```
kges=[ 3.5836e+000    9.6253e+002    7.4892e+000 ...
```

```

        1.3713e+003    1.9785e-001    1.0173e+003 ...
        7.3255e+000    1.3737e+003    1.2872e+003 ...
        2.2830e+003    1.6335e+002    8.8603e-005 ...
        9.7711e-003    2.5870e+002    9.8598e-003 ...
        7.2555e+002    1.0202e-002    1.7334e+004 ...
        1.0272e-002    3.3505e+002    5.5920e+004 ...
        6.4040e+004];%ss=3016
k0=kges;
ra=rand(1,22); k0=kges.*(0.75+0.5.*ra);
for ii=[1:10];

k0=log(k0);
[x fval]= fminsearch(@zielfunktion,k0,options)
ZWISCHEN=[];
ra=rand(1,22); k0=kges.*(0.75+0.5.*ra);
end;

```

#### 4.2.5 zielfunktion.m

The MATLAB function `zielfunktion.m` is called by the optimization routine as the objective function. Here the sum of the squared relative errors is calculated. The calculated concentrations are obtained by calling the function `caus.m`

```

function f = zielfunktion(x)
global DATEN ZWISCHEN IMESS;
x=exp(x);
nsub=9 ;ngl=10;
%k0=1000*eye(1,10);
%k0(9)=x(1);k0(10)=x(2);
f=0.0;
for i=[1 : 266]
    IMESS=i;
    k0=x(1:ngl);
    oo=x(ngl+1);
    deltat=x(ngl+2);
    T=DATEN(i,2);
    t=DATEN(i,4)-deltat;
    ea=x(ngl+3:ngl+ngl+2);

% kennnummer kelvin druck zeit fco fh2o fh2 fco2 co co2 h2 h2o

```

```

%      1      2      3      4      5      6      7      8      9      10      11      12
%y( 1) = CO
%y( 2) = CO2
%y( 3) = H2
%y( 4) = H2O
%y( 5) = Z
%y( 6) = Z_CO
%y( 7) = Z_CO2
%y( 8) = Z_H2
%y( 9) = Z_H2O
    c0=[DATEN(i,5) DATEN(i,8) DATEN(i,7) DATEN(i,6) 0 0 0 0 oo ];
    c=caus(nsub,ngl,c0,t,T,k0,ea);
    f=f+(100*(DATEN(i,9)-c(1))/(DATEN(i,5) +DATEN(i,8)))^2;
end
hv=[f x];
ZWISCHEN=[ZWISCHEN;hv];
fid = fopen('lauf2002072222.txt','a');
fprintf(fid,'%20.8e',hv);
fprintf(fid,'\n');
fclose(fid);
%sprintf('Fehlerquadratsumme = %15.5f',f)

```

#### 4.2.6 caus.m

The MATLAB function `caus.m` is called by the objective function `zielfunktion.m`, it calculates the reaction rate constants from the Arrhenius parameters and calls the differential equation solver.

```

function c = caus(nsub,ngl,c0,t,T,k0,ea);
global DATEN IMESS;
for i=1:ngl
    k(i)=k0(i)*exp(-ea(i)/(8.3145*T));
end
%options = odeset('RelTol',1e-5,'AbsTol',1e-8);
options=[];
[tt,y]=ode15s(@dgl,[0 t],c0,options,k);
c=y(length(y),:);

```



## References

- [1] A. D. Overstreet. A screening study of a new WGS-catalyst. Master's thesis, Virginia Polytechnic Institute and State University, Blacksburg, Virginia, USA, 1974.
- [2] V. Berispek. Studies of an alkali impregnated Co-Mo-catalyst for WGS and methanation. Master's thesis, Virginia Polytechnic Institute and State University, Blacksburg, Virginia, USA, 1975.
- [3] Carl R. F. Lund. Microkinetics of water-gas shift over sulfided Mo/Al<sub>2</sub>O<sub>3</sub> catalysts. *Ind. Eng. Chem. Res.*, 35:2531–2538, 1996.
- [4] Carl R. F. Lund. Effect of adding Co to MoS<sub>2</sub>/Al<sub>2</sub>O<sub>3</sub> upon the kinetics of the water-gas shift. *Ind. Eng. Chem. Res.*, 35:3067–3073, 1996.
- [5] Yumin Li, Rejie Wang, and Liu Chang. Study of reactions over sulfide catalysts in CO-CO<sub>2</sub>-H<sub>2</sub>-H<sub>2</sub>O system. *Catalysis Today*, 51:25–38, 1999.
- [6] P. Hou, D. Meeker, and H. Wise. Kinetic studies with a sulfur-tolerant water gas shift catalyst. *J. Catal.*, 80:280–285, 1983.
- [7] R. Hakkarainen, T. Salmi, and R. L. Keiski. Water-gas shift reaction on a cobalt-molybdenum oxide catalyst. *Appl. Catal., A*, 99:195–215, 1993.